Optical studies of wrapgated InP nanowire arrays

Henrik Torstensson

October 6, 2019

ABSTRACT

This thesis describes optical spectroscopy on III-V semiconductor InP nanowires (NW) with a transparent indium-tin-oxide (ITO) gate electrode. The Nws are arranged both as vertical arrays with a wrap all around gate and as single lateral NWs with an omega-shaped gate for increased electrostatic effect.

The transparent ITO gate allows optical access with probing lasers in a 4 K He-cryostat while controlling the electrostatic environment with the gate. A coldfinger is constructed to provide easy access when connecting the samples in the cryostat.

Photoluminescence (PL) spectroscopy is used to investigate different effects in the NW. A large blueshift (110 meV) in peak energy is seen with increasing excitation power in p-doped samples but only a small shift of 10 meV is seen in n-doped. A model is proposed where this is explained with statefilling and the effective mass being different in the conduction band compared to the valence band.

A model by Chia and LaPierre is implemented and expanded to gate bias. It uses density of interface traps (D_{it}) to explain how the band bending and depletion in the NW changes with radius, surface defects and bias.

ACKNOWLEDGEMENTS

This thesis was long in the making and I could not have pulled it off without the help from of others.

Most importantly Dan's open door and endless patience at all stages of this project kept my hopes up. My supervisor Gustav must have grown a small forest of nanowire arrays and showed me that when life gives you faulty devices you double down and reiterate your way past problems.

David and Kilian for not only showing me how to operate the setup but knowing what to fix when the lab troll got loose. Carina for delivering a fantastic introduction to solid state physics where diamonds the size of the earth where par for course.

Anthony for reading the thesis and giving valuable comments and encouragement, Simon for sharing long hours in the salt mines, Anita for well needed reminders and coaching. And finally Kajsa for being the perfect support team.

POPULÄRVETENSKAPLIG SAMMANFATTNING

Att manipulera elektronpopulationer

Jag har undersökt hur en genomskinlig omslutande elektrisk kontakt kan påverka antalet elektroner i nanotrådar och användas i jakten på ett optiskt fenomen kallat excitoner där elektroner och positiva hål binder ihop till ett väteatom-likande tillstånd.

Elektroniken har revolutionerat våra liv och dess viktigaste komponent är transistorn. Redan från början var miniatyrisering den främsta drivkraften i utvecklingen, och den har gått i rasande tempo sedan dess. Transistorerna blev snabbt ihopkopplade i integrerade kretsar och från att ha haft en handfull i en radio 1954 så finns det ca 1 biljon transistorer i en smartphone 2019. Moore's lag som beskriver den här snabba utvecklingen har länge levt på att man har kunnat skala ner kiselkomponenter med finurliga metoder. Den relevanta storleken är gate-längden som nu är nere på 5 nm vilket motsvarar ca femtio atomer. Här verkar det dock som att det börjar ta stopp, kvantfysikaliska effekter som inte spelar någon roll på större skala blir allt viktigare ju mindre komponenter blir. I små kretsar så börjar elektronerna tunnla genom barriärer som de inte kommer igenom enligt klassisk fysik och det uppstår stora läckströmmar. För att fortsätta beräkningsutvecklingen med snabbare och snålare transistorer så utforskas andra material och geometrier för fullt.

Nanotrådar

Nanotrådar (eng nanowires) är små halvledarpelare med en tjocklek under tiotals nanometer som ofta är några mikrometer långa, de är alltså mindre än en tusendel så tjocka som ett hårstrå. De små dimensionerna tillåter bland annat blandningar av material som vanligen inte passar ihop på grund av mekaniska spänningar. Ett sådant är indiumfosfid (InP), en förening av två ämnen från grupp III och V i det periodiska systemet. InP är mycket mer lämpat för elektrontransport än vad kisel är både i motstånd och snabbhet att reagera på förändringar i elektrisk spänning. Det är dessutom synnerligen väl lämpat för komponenter som producerar ljus.

På gott och ont blir yteffekter väldigt stora i en nanotråd men till skillnad från vanliga transistorer kan man lägga en elektrisk kontakt kring hela omkretsen istället för att påverka endast från en sida. Här har vi valt att använda en genomskinlig elektrisk kontakt av materialet ITO (vanligt i pekskärmar i smartphones) för att kunna undersöka vad som händer med både elektriska och optiska metoder samtidigt.

Det visade sig att den genomskinliga kontakten påverkade ytan i nanotråden på ett oförutsett sätt som störde möjligheten att skapa excitonen. En datorsimulering antyder att störningar vid gränsen mellan nanotråden och kontakten är nog för att sabotera det vi tänkte mäta. För att minska störningarna föreslås ett passiviserande lager läggas mellan nanotråden och dess omgivande ITO kontakt och på sätt minska interaktionen mellan ITO och ytan.

CONTENTS

1

THEORY

1.1 INTRODUCTION

Nanowires (NWs) are manufactured structures with thickness on the order of nanometers (nm) making them behave differently than their bulk counterparts. The small dimensions make it possible to combine materials with otherwise incompatible lattice structures as the strain can relax radially over the thin NWs [1] and finally, for really thin ($\sim$ 10 nm) NWs, the effects of quantum mechanics become important. The large surface to volume ratio also makes the physics of the surface much more dominant than in bulk materials.

The surface effects are sometimes detrimental to the properties that are desired in nanotechnology. To minimize the surface effects we use a material known for its passive surface [2], indium phosphide (InP), as material for the NWs. It's a III-V material, a compound material from chemical group III and V, these two elements combine and create a semiconductor with a direct bandgap with an energy close to visible light and a surface that allows few non-radiative recombinations (good optical properties). As a bonus it also has fast electrical response because of its low effective mass for electrons.[3] A downside that became apparent in the thesis is that the low surface recombination rate quickly degrades when some materials are deposited onto the InP.[4]

1.2 MOTIVATION

The goal is to test the feasibility of a setup to spatially separate excitons seen in figure 1. An exciton is a quasi particle that consists of a bound electron and hole pair. The negative and positive particles can form a hydrogen atom like bound state with a slightly lower energy than the sum of its parts [5]. If the Fermi level can be closely controlled across the bandgap with an electrostatic potential, charge carriers could be injected without the irreversible addition of dopants. The charges could then be brought into close proximity on either side of a potential barrier. Excitons could then form and hopefully last much longer since they are more unlikely to recombine when separated in space. The NWs are also known for allowing to grow a defect free crystal heterostructure that prevents the excitons to recombine through a defect[6]. Being

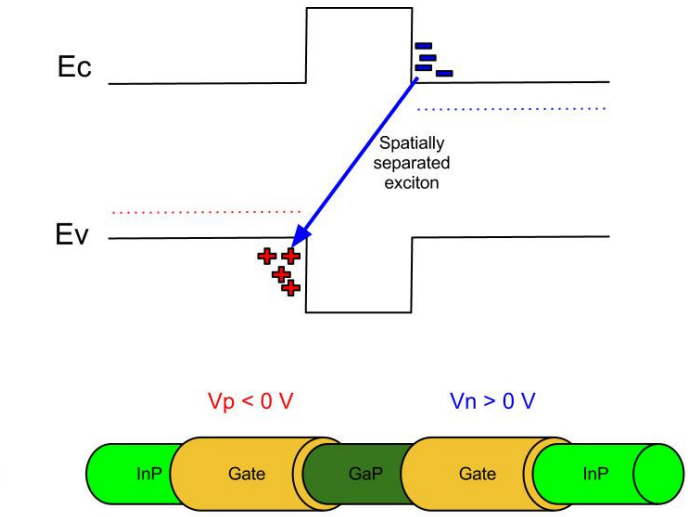

Figure 1.: Schematic of how we want to realize the separated excitons and accompanying simplified band structure. The transparent gate should give a strong control over the charge carriers since it wraps all around a small volume. Electrons and holes can form excitons without interference from dopants. The dotted lines represent the Fermi-level.

bosons, the excitons could then be used to study Bose-Einstein condensates (BEC) [7], quantum computing [8] and photonics in general.

As a first step I will use photoluminescence spectroscopy (PL) to study what happens when InP nanowires are coated in a transparent gate to control the electrical potential. This wrap-gate should offer a higher control of the charge carrier concentration compared to a planar geometry [9] and hopefully allow us to control the Fermi level across the bandgap. As we shall see later I never got past the first stages and instead focused on how and why the NWs luminesced depending on radiu, doping and exciting intensity. The spatially separated exciton stayed a distant goal.

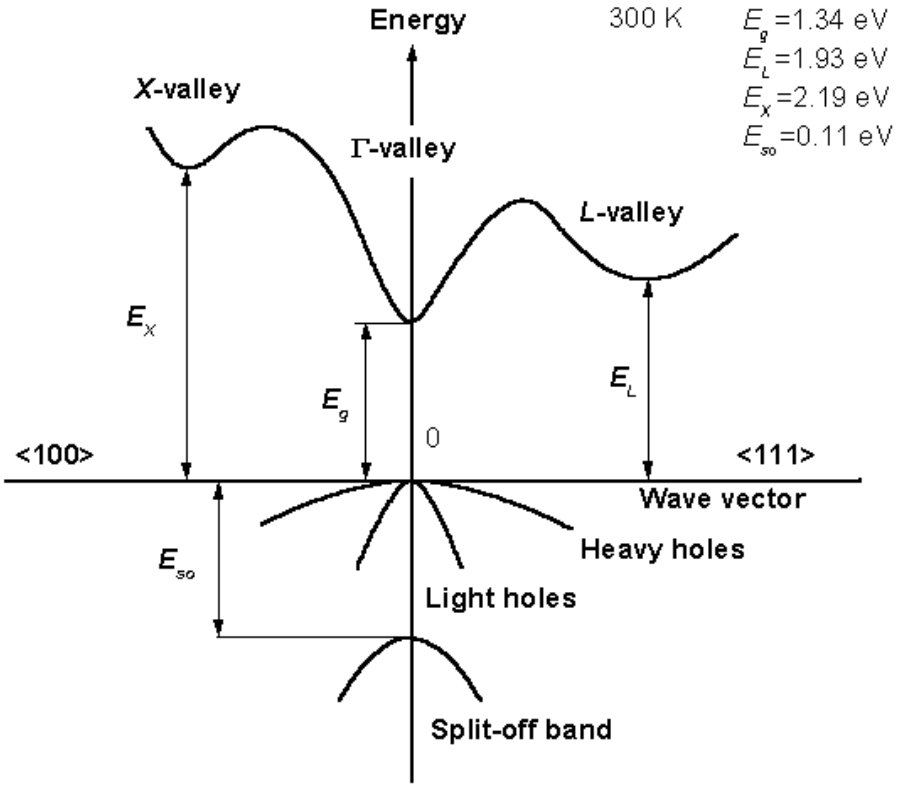

Figure 2.: Band structure in **k**-space for InP. Notice the direct bandgap where the Γ-valley and hole peak is aligned vertically and allow likely optical transitions. (Image from chapter 8 of [11])

1.3 THEORY

Some materials form crystals, where the atoms are placed in a periodic structure. When electrons travel through the structure they are forced into certain available energy states created by the periodic crystal. This forms bands with permitted states separated by bands of forbidden energies.

Given the periodic structure of the crystal and the electron waves it is sometimes useful to speak of their wave vector **k** which is related to how fast the wave function oscillates and in which direction it is travelling. Assuming that the particle is travelling in a periodic potential gives the bands a shape seen in figure 2 that can be approximated by parabolas ($E = E_0 + \frac{\hbar^2 k^2}{2m_e}$) close to band minima and maxima in **k**-space. Together with the Fermi level this explains many of the electrical and optical properties of a material. [10]

Since two electrons can't occupy the same state they fill the available states (if undisturbed by for example lattice vibrations) from the lowest energy and up.

The topmost occupied band in a semiconductor is called the valence band. Above the forbidden bandgap lies the empty conduction band without electrons. If an electron is excited with more energy than the bandgap it can reach the conduction band where a current can be transported. It will leave behind a hole in the valence band that can be treated as particle with positive charge.

We can permanently add electrons to the conduction band by replacing every millionth or so atom with a similar atom with an extra charge carrier (dopant) to the crystal. This will not change the overall structure but when the dopants are ionized by heat and release their charge carrier we can precisely control the charge carrier concentration. Depending on the dopants chosen we can create extra electrons (n-doped) or holes (p-doped). [10]

1.4 PHOTOLUMINESCENCE SPECTROSCOPY

A technique used to investigate parts of a band structure is photoluminescence spectroscopy (PL) [12]. The physics is illustrated in figure 3. When a photon with energy (E_{exc}) larger than the bandgap E_g is absorbed it creates an electron-hole pair. The electron then relaxes through lattice vibrations, fast non-radiative processes, to a state with lower energy, usually the conduction band edge or an even lower state such as excitons or donors and then ideally to the valence band through radiative transition by spontaneously emitting a photon with energy E_{PL}. The hole relax to the top of the valence band and recombine with an electron.

In a direct bandgap the minimum of the conduction band and the maximum of the valence band align in k-space (see figure 2), meaning there is no need for phonons [13] to assist in the transition as momentum must be conserved and photons have almost zero momentum and therefore making it more likely and efficient for optical purposes. Competing with this ideal process are impurities and surface states that can create energy levels in the middle of the bandgap that can facilitate non-radiative recombinations.[14] [15]

A theoretical spectrum of spontaneous emission without defects will have an intensity form $I(E)$ governed by combining the Boltzmann distribution and the density of states into equation (1)

$$I(E) \propto \sqrt{E - E_g} \exp\left(-\frac{E}{kT}\right) \tag{1}$$

and will as a consequence have a peak at $E_g + 1/2kT$ where k is Boltzmanns constant and T is the temperature.[14]

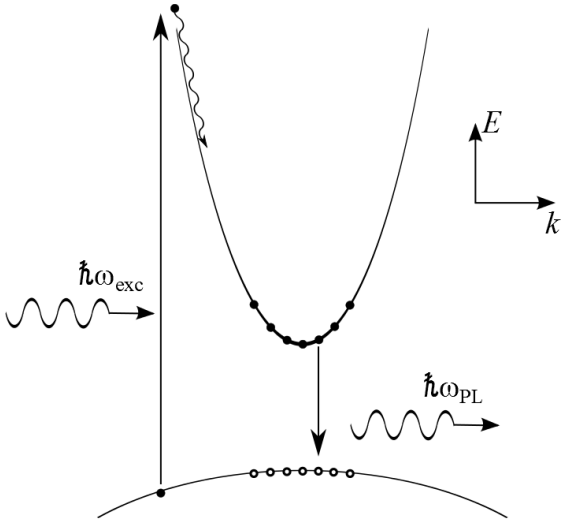

Figure 3.: Ideal photoluminescence with direct bandgap allowing efficient transitions.

When under powerful excitation the sample can sometimes heat up so it is useful to know the temperature dependence of the bandgap as seen in equation (2). We can see that increasing temperature will narrow the bandgap. [11]

$$E_g(T) = 1.421 \text{ eV} - 4.9\Delta 10^{-4}\Delta T^2/(T + 327 \text{ K}) \text{ eV} \tag{2}$$

PL gives information about the bandgap energy and some information about charge carrier density. It can also be used in other experiments to see and interpret the lifetime of charge carriers as well as polarization and intensity of light given the right setup.[16]

1.5 STATE FILLING AND EFFECTIVE MASS

Electrons and holes can be attributed an effective mass m_e depending on how easily they can be accelerated in different materials. In **k**-space this mass can be visualized as flattening of the parabolas, heavy mass means flat bands and light mass means a more arched curve. [17]

All states are distributed by the same distance along the k-axis so a specific amount of heavy charge carriers can be contained in a small energy span while the same amount of light carriers would be spread out over a large energy (visualized in figure 3). In InP electrons in the conduction band at the Γ point, the bottom of the conduction band in this material, have an effective mass of 0.077 m_e see figure 2 [11]. The low mass is also one of the reasons that III-V materials are of such interest in electronics, they can react faster to change in gate bias [18].

In the state filling regime where electrons are added to the conduction band we get a situation similar to a metal where E_F is in the conduction band. This can be treated

as the lowest available energy state is the bottom of the conduction band. The number of charge carriers at an energy is given by the Fermi-Dirac-distribution $F(E)$ and the density of states ($Z(E)$) for the system see equation (3). When the thermal excitations (kT) are small compared to E_F (measured from the bottom of the conduction band) the energy states are filled from their lowest level to close to E_F. There thermal excitations leaves some states below E_F unoccupied according to equation (3).[14]

$$F(E)Z(E) = \frac{1}{e^{(E-E_F)/kT}+1}Z(E) \tag{3}$$

At low temperatures when $kT << E_F$ the behavior of the electron population is dominated by the Pauli principle. The electrons cannot occupy the same state so if the population is large in a band the electrons fill up and occupy all the available states in the bottom of the band. No photons can be excited to the occupied states so in an absorption experiment the bandgap would appear to be larger since the bottom of the band is already occupied. This apparent blueshift is called the Burstein-Moss (BM) effect. [19] Large filling can be achieved by anything that puts many charge carriers in a band at a relatively low temperature for example heavy doping [20] or high optical excitation intensity in some systems. The semiconductor is called degenerate if E_F is in the conduction band for n-doped or in the valence band for p-doped samples.

At low temperatures and degenerate doping the energy shift ΔE from the BM effect has a relationship with the charge carrier concentration according to equation (4). [21]

$$\Delta E = \frac{\hbar^2}{2m_{eff}}(3\pi^2 n)^{2/3} \tag{4}$$

Here n is the concentration of electrons in the conduction band.

1.5.1 *Model statefilling with minority effective mass*

When estimating the state filling one has to take into account that recombination increases with increased electron-hole population. I am going to make a bold assumption that however the minority carriers reach their steady state distribution in n- and p-doped samples, they do it in the same way. So a given excitation power should result in the same number of added charge carriers in a p-doped sample as an n-doped sample. In figure 4a we focus on an n-doped sample. The doping has filled the bottom of the conduction band with electrons so the recombination is mostly governed by the minority population of holes. When more holes are added through increased excitation intensity the low temperature and the Pauli principle will stack the holes from the top of the valence band. The density of states is inversely proportional to the effective mass.

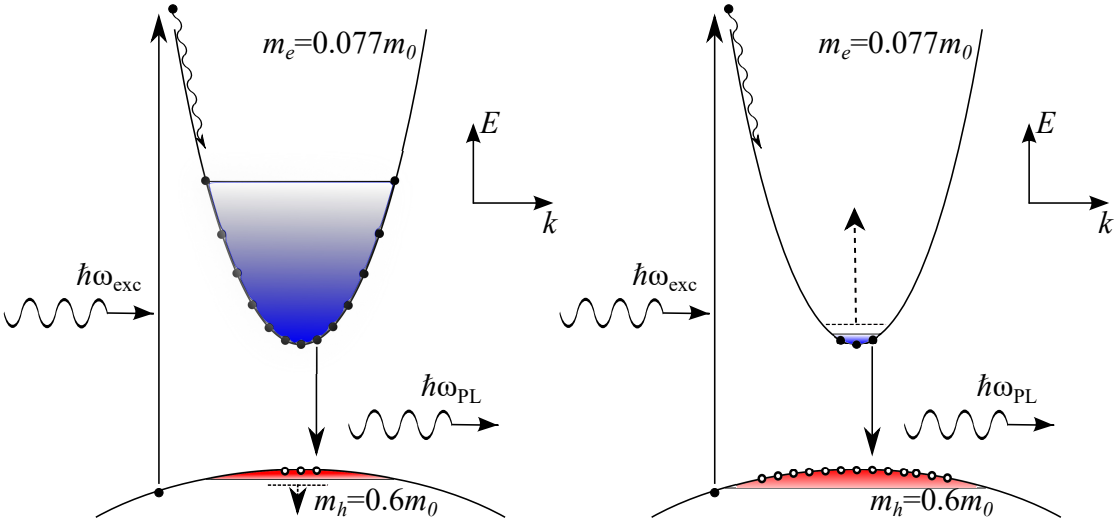

(a) n-doped (b) p-doped

Figure 4.: Schematic of degenerately doped InP in **k**-space. The dashed arrows represent the relative speed at which the band fill up when charge carriers are added. (a) The blue filling in the conduction band represents filled electron states from doping and laser excitation and is much larger than the filled hole states in the valence band from laser excitation. Since the recombination is limited by the hole population the energy spectrum will also be governed by them when photogenerated charge carriers are much fewer than dopants. So an increase in excitation intensity should blueshift the PL-spectrum inversely proportional to the minority carrier mass, the holes for n-doped InP. (b) In the p-doped sample there is instead an abundance of holes. They are distributed closer in energy so the shaded red area is smaller. Here the photogenerated electrons are the minority charge carriers. The dashed arrow is longer here to indicate the larger increase in energy with each added electron due to lower effective mass compared to n-doped samples.

This should mean the peak energy shift is inversely proportional to the effective mass of the minority charge carriers when the same exciting power is used in heavily doped samples, see equation (5).

$$\Delta E \propto \frac{1}{m_{effminority}} \tag{5}$$

The assumption glosses over many things that are different between holes and electron, for example that the band bending at the NW surface is different in p-doped and n-doped samples and will leave the electrons in the center or close to the surface.

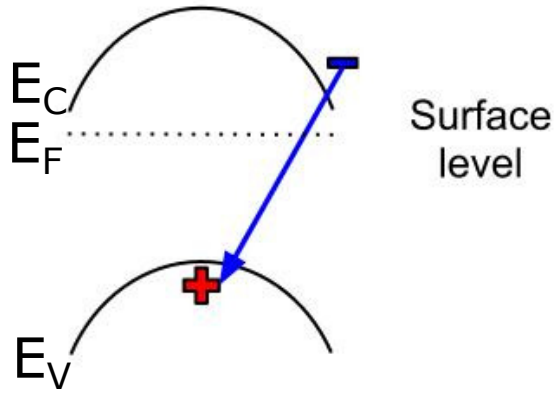

Figure 5.: Band bending in the cross section of a NW and resulting separation in space of electrons and holes.

A more conservative statement is therefore that I at least expect the peak shift to be smaller in n-doped samples than in p-doped samples.

Another prediction based on figure 4a is that the spectrum for n-doped samples should have a peak at higher energy and start with a wider peak that shifts slowly with increased excitation intensity since the electrons occupy a wide range in energy. Based on figure 4b p-doped samples with the same doping concentration should start with a narrower peak with lower energy and both quickly shift to a broad peak and higher energy.

1.6 BAND BENDING

At all crystal interfaces there can exist space charges that locally change the band structure away from that of the bulk. These space charges can arise from the sudden change in crystal structure at the surface that leaves dangling bonds and need for charge neutrality. So the bands bend to accommodate the Fermi level in the bulk and at the surface. This leaves a depletion depth w with practically no charge carriers illustrated in figure 6. In a planar n-doped semiconductor with applied bias V, w can be calculated with equation (6) if one can find the built in potential ψ_{bi} [14].

$$w = \sqrt{\frac{2\epsilon_s}{qN_D}(\psi_{bi} - V - \frac{kT}{q})} \tag{6}$$

[10] In a NW this bending can extend through the entire volume since the surface is always close, this leads to a spatial separation of holes and electrons that decreases the probability of them recombining radiatively seen in figure 5.

The infinite crystal approximation used to calculate the forbidden states of the bandgap is clearly violated at the crystal interface. At the surface some localized states are allowed in the bandgap. Especially when in contact with a metal (illustrated in figure 6) there will arise interface states in the bandgap that act as acceptors close to the conduction band or donors close to the valence band, they are known as metal induced gap states [22]. At some level there will be a charge neutral level (CNL) and we can treat the entire surface as having an effective density of interface states D_{it}, neutral full donors below, and neutral empty acceptors above. If the Fermi level is below CNL the donors will become positively charged and if above the acceptors will be negatively charged and counteract some of the Fermi level change. With a large D_{it} the Fermi level can only be shifted a small distance energy-wise regardless of applied bias, doping or different work functions of neighboring materials [23] since the change adds so many new counteracting charges. The surface potential will be pinned to the CNL. The degree of pinning depends on the size of D_{it}, it is not a binary state [14].

During a PL measurement the created electron-hole pairs will be separated to the surface and core by the band bending. The recombination will slow down and the energy will be lower than the bandgap. Higher excitation intensity will create more separated electrons and holes that neutralize and overcome the bending from the dopants and flatten the bands. This leads to higher PL energy and a higher probability of recombination as the electrons and holes can exist closer in space as illustrated in figure 7 [24].

1.7 RATE EQUATIONS

Now when we have determined how to generate charge carriers in the bands it is time to take a closer look on how fast they recombine to produce light.

The recombination rate R is determined by the charge carrier concentrations n, p and the probability to recombine A. Excitation creates electron-holes pairs so added electrons $\Delta n =$ added holes Δp.

The equilibrium electron and hole concentrations n_0 and p_0 $n = n_0 + \Delta n$ $p = p_0 + \Delta p$

$$R_{opt} = Anp = A(n_0 + \Delta n)(p_0 + \Delta p) \tag{7}$$

With n-doping the majority equilibrium population is much larger than the optically generated when the excitation is small see (8).

$$n_0 >> \Delta n \tag{8}$$

For the holes the opposite is true

$$p_0 << \Delta p \tag{9}$$

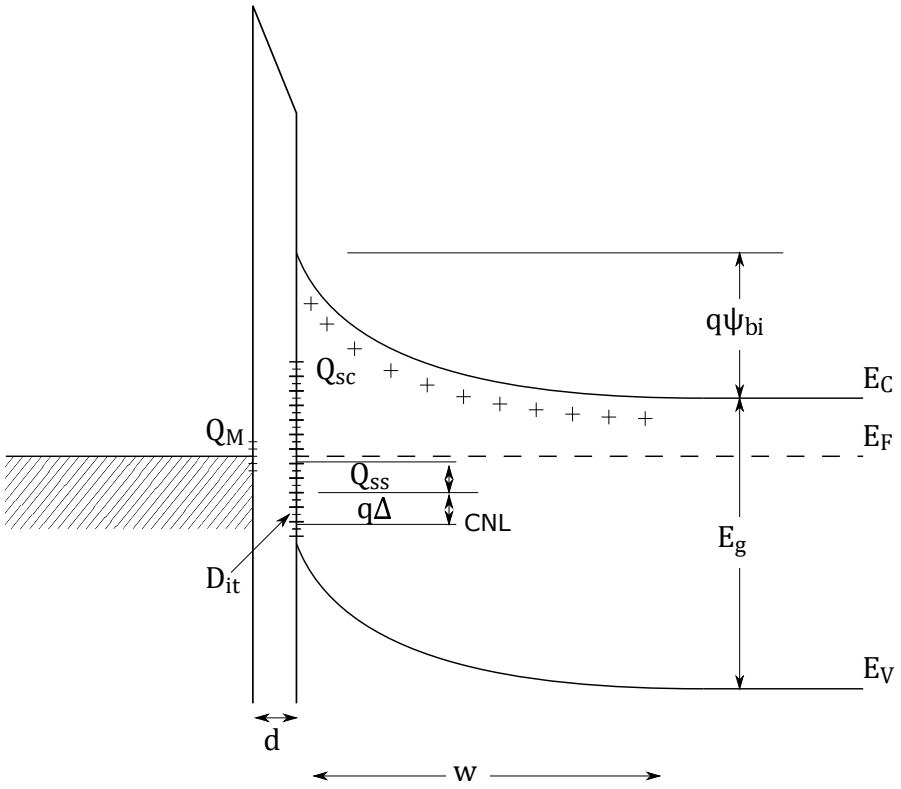

Figure 6.: Band diagram of metal-n-semiconductor contact with an interfacial vacuum layer with distance d. The Fermi levels E_F have aligned and caused a space charge $_{SC}$ in the semiconductor with width w free of electrons. The charge Q_{ss} and $q\Delta$ is caused by the Fermi level being above the CNL and inducing charges from the interface states D_{it}. [14]

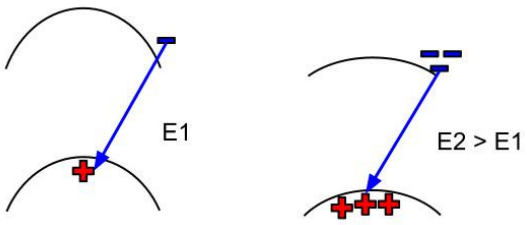

Figure 7.: Band bending in cross section of NW overcome by added charge carrier population. This increases radiative recombination rate and increases the apparent bandgap.

We arrive at

$$R = Anp = A(n_0 + \Delta n)(p_0 + \Delta p) = An_0\Delta p \tag{10}$$

So we expect the recombination rate R and thus the PL intensity to be proportional to the pumping laser intensity I_L or added charge carriers if non-radiative recombinations are small and the excitation intensity isn't too big.

Another way to describe it is that two processes that compete in the recombination is the non-radiative recombination through defects states known as Shockley-Read-Hall (SRH) recombination and the band to band recombination. SRH involves a single charge carrier so the recombination is proportional to N whereas band to band recombination involves both an electron and a hole and is thus proportional to N^2.

The PL intensity I_{PL} is described in equation (11),

$$I_{PL} \propto N^2 \tag{11}$$

The absorption from the laser intensity I_L is described in (12),

$$I_L \propto A_1 N + B_1 N^2 \tag{12}$$

where A_1 and B_1 are constants.

By combining equation (11) and (12) we get an expression for the combined recombination processes of both radiative band to band recombination and through nonradiative defect recombinations

$$I_L = C(AI_{PL}^{1/2} + BI_{PL}^{1}) \tag{13}$$

where C is a material and geometry based constant.

In a power relationship the exponent a in equation (14) should be close to 1 if the recombination is dominated by band to band processes. In a similar manner one can arrive at an exponent value $a > 1$ if non-radiative recombinations are dominant [21].

$$I_{PL} \propto I_L^a \tag{14}$$

1.8 MODELLING WRAPGATE

The experiment changes many variables so to get some sense of what might happen a simulation is made using the finite element method software Comsol and its semiconductor module. It uses the drift diffusion equation and can model electrostatics and transport including recombinations. A limitation is that it doesn't include any quantum mechanical computations and is optimized for structures larger than 100 nm (as opposed to my oxide of 10 nm).

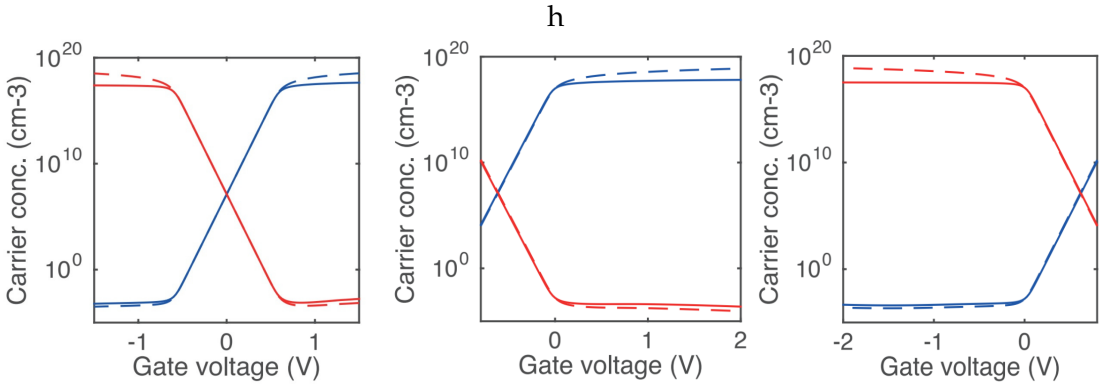

Figure 8.: From left to right: Simulation of charge carriers in i-, n-, p-doped InP NW with radius=25 nm and gate oxide=10 nm. Blue lines are electrons and red holes. Dashed lines are average concentration, solid lines are concentration in the core of the NW. (G.Nylund)

The structure is made up of a cross-section of an InP nanowire connected to electrical ground and wrapped with a thin gate oxide and a metal to simulate the ITO. The spacer is made of an insulating surface.

An interesting property for us is how the charge carriers react to gate bias, this is seen in figure 8.

It is highly dependent on doping level and we should expect this from our experiments as well. But apart from the type of majority charge carrier and that we need to flip the bias polarity p- and n-doped samples should behave the same according to this simulation.

The simulation does not take into account the pinning from the interface states D_{it} or whether a Schottky diode contact forms with the substrate or gate oxide.

1.9 MODELLING SURFACE DEPLETION

To establish the effects of surface interface defects D_{it} and shed some light on how radius dependent the band bending in the NW is I implemented a model in Matlab. An illustration of what we are modelling is shown in figure 9.

The gate oxide HfO_2 has been known to cause surface defects at the interface to semiconductors so a model with D_{it} seemed doubly important. [25]

The modelling was heavily influenced by the articles [26] and [27], changes were made in material properties and the addition of surface charges from gate bias.

The method can be summarized as follows. Poisson's equation in cylindrical coordinates gives two solutions, a partially depleted NW and a fully depleted NW. In the partially depleted NW determine charge density ρ based on doping then determine

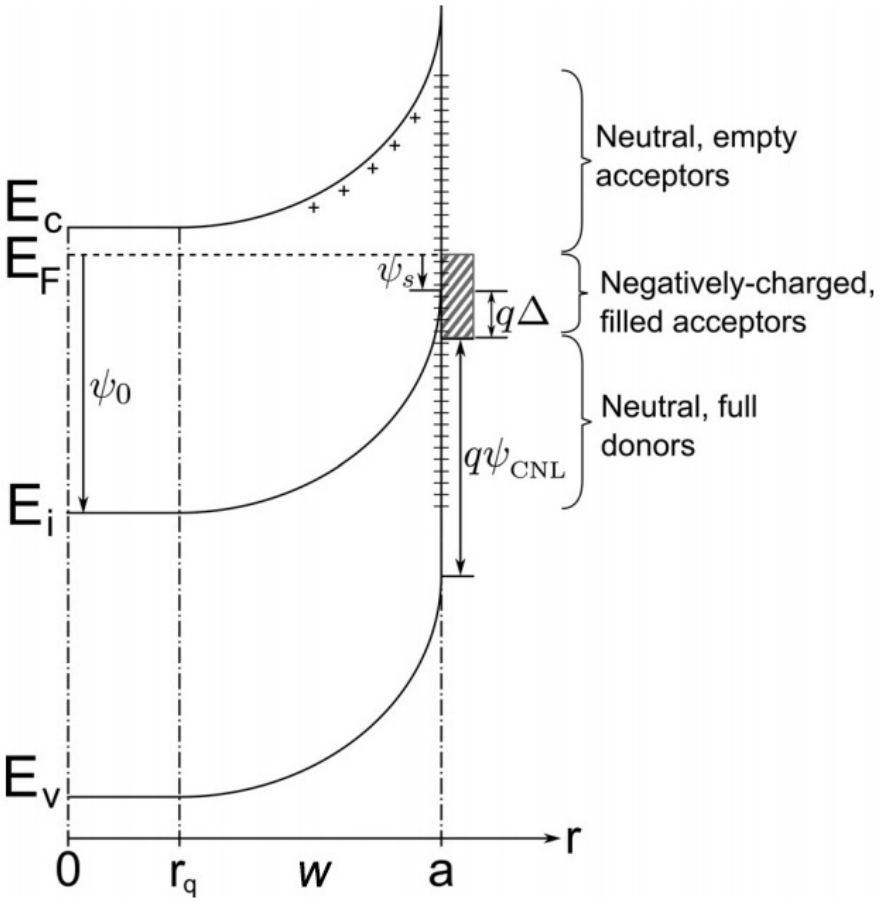

Figure 9.: Band diagram along the cross section of a NW. The interface states D_{it} are visualized as acceptors and donors at the radius a. Since the charge neutral level (CNL) is below the band midpoint E_i the interface states act as negatively charged filled acceptors and cause a charge $q\Delta$ that pins the band closer to the CNL. (Image by Chia et al with an added w to indicate the depletion width.)

the potential at the center of the NW ψ_0 and the radius from the center that is not depleted r_q. This gives the full potential $\psi(r)$.

In the fully depleted NW $r_q = 0$ so determine ρ and ψ_0. This gives the full potential $\psi(r)$.

A more elaborate explanation of the method [26] to find the NW potential $\psi(r)$ is shown in appendix A. There I have also outlined the changes I have made in equation (28) to model the addition of surface charges from gate bias.

2

STRUCTURES AND SETUP

2.1 STRUCTURES

Mainly two types of structures were investigated, arrays of vertical nanowires with ITO wrap gates and single lateral nanowires with ITO omega gates.

2.1.1 *Arrays*

The initial experiments were performed on arrays of vertical InP NWs seen in figure 11. These arrays consist of ordered matrices of 200 by up to 800 NWs. The diameter of the NWs is the same ($\pm$ 1 nm) within each array and each sample has several matrices with diameters ranging from 40 to 70 nm and a length of roughly 2 μm capped with a gold seed particle. A more detailed view of the NW dimensions are found in figure 10.

Around the nanowire is a 10 nm gate high-k dielectric (HfO_2), high k materials allow us to keep a high capacitance from gate to NW while making the oxide thick enough to prevent gate leakage and breakthrough. The outer layer is a 30 nm wrap-gate of indium tin oxide (ITO).

At the base of the nanowire is a sheet of light blocking metal (W or Au) so that the signal from the NWs is not lost or confused in the background from the substrate.

Samples were grown with 5 levels of doping (n+, n, i, p, p+) to test the response of the gate.

Type	Dopant	Concentration (cm^{-3})
n+	S	$2 \cdot 10^{18}$
n	S	$2 \cdot 10^{16}$
undoped		
p	Zn	$\sim< 10^{16}$
p+	Zn	$\sim< 10^{18}$

Table 1.: Different dopants used in our NW growth. It is very difficult to estimate the p concentration. (J. Wallentin)

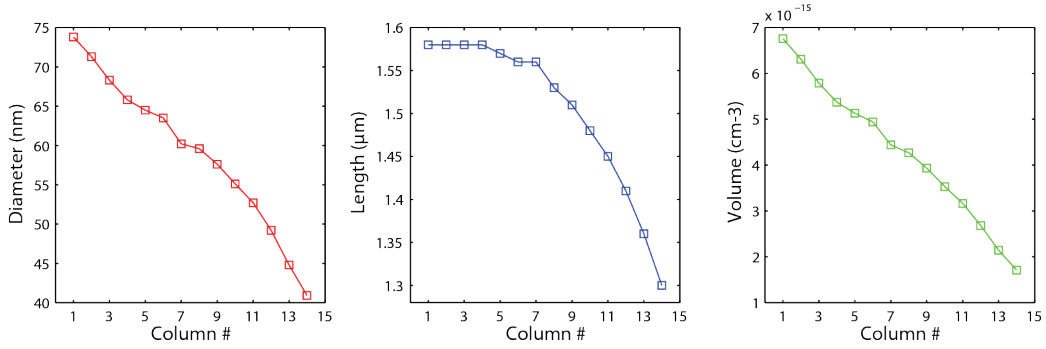

Figure 10.: NW dimensions in a typical array, measured in SEM. Ideally the length should be the same but is prevented by the physics behind growth. The arrays where seeded in a matrix form with identical rows and differing diameters in each column to give many testable devices on each sample. Figure 11c shows one array from all the rows and columns. (G.Nylund)

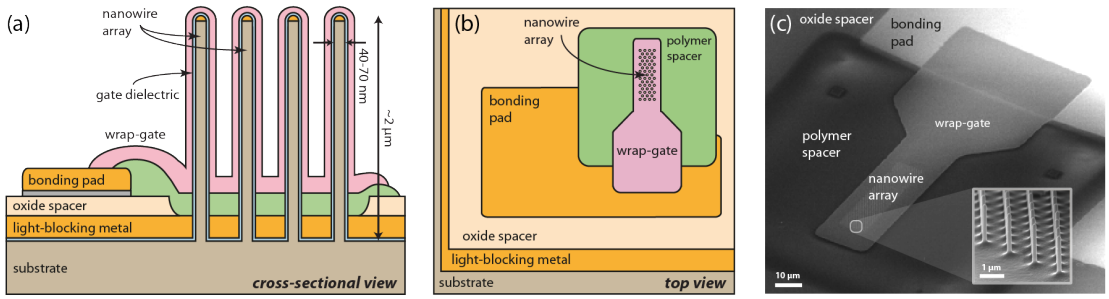

Figure 11.: Schematic of vertical NW arrays. In figure c an array of NWs is seen. All the NWs in the array have the same diameter. On a sample there are many such arrays with different diameters according to figure 10 (G.Nylund)

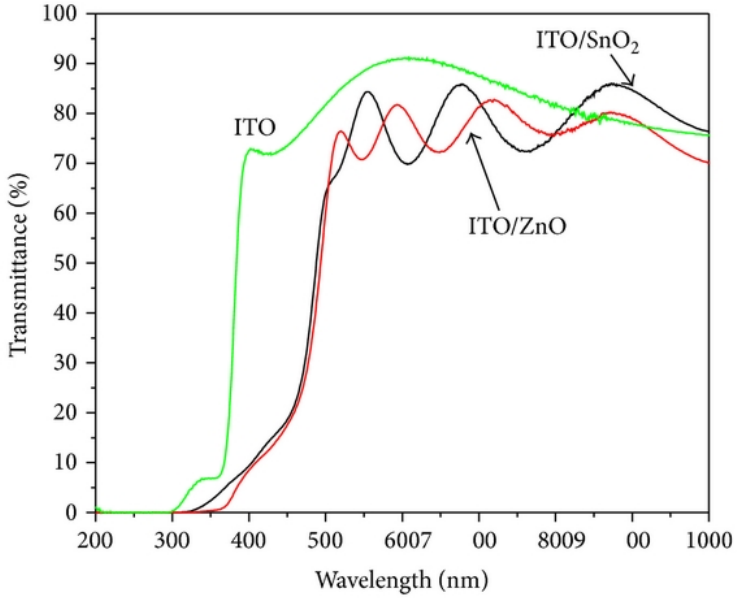

Figure 12.: Transmittance for ITO thin film. Also transmittance when interfaced with other oxides for reference. Not the same material but shows that the transmittance can by drastically altered depending on interfaces with other materials. (Tingliang Liu et al) [30]

2.1.2 *Wrap-gate*

As the name implies a wrap gate covers the entire surface of the nanowire, this will hopefully increase the capacitance and thus the control over charge carriers. The idea of an all around gate is not new and has been realised before [9] but we want to use optical measurement techniques so the gate has to have high transmittance.[28] ITO is chosen for the gate material as it is mostly transparent in thin films (50-90 %) in the wavelength-region 500-1500 nm (see figure 12) while at the same time being a good electrical conductor, it's not a metal but so heavily n-doped that it acts metallic.[29]

The transmittance is in part explained by the bandgap of a material, photons can't be absorbed if their energy is lower than the energy required to excite electrons across the bandgap. As we will see later in section 3.1.2 and 3.3.3, it turned out that the ITO gate is not simply a transparent gate but interacts with the luminescence and interface states, especially with the p-doped NWs.

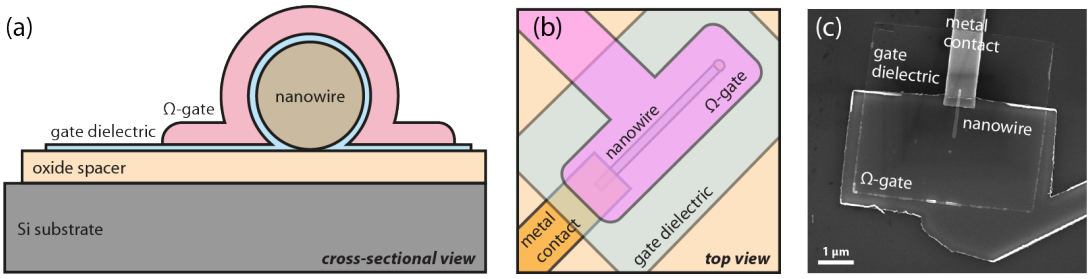

Figure 13.: Schematic of the lateral NW. (G.Nylund)

2.1.3 *Single nanowires*

Nanowires from the array samples before gate dielectric and ITO are added are broken off with a tissue and transferred to a new SiO_2 covered Si substrate. It is connected with a gold EBL line and then covered with gate dielectric (HfO_2) and an ITO gate. An illustration of this is found in figure 13. The gate does not completely surround the NW but the Ω shape should be a close approximation of a wrap gate and has successfully been demonstrated in [31].

2.2 GROWTH

The NWs were grown (by Jesper Wallentin) using metal organic chemical vapor deposition (MOCVD) in which gold particles are seeded on a substrate in the desired matrix shape and act as a catalyst for a gas. The different gas molecules deposit atoms that self-assemble on the preexisting crystal structure under the gold particle and slowly build a NW from the bottom up.

Gustav Nylund did the seed particle pattern and remaining processing on the samples, from gate oxide to bonding the samples. For more technical details about the growth and processing see [28].

2.3 COLD FINGER

The measurements had to be done at low temperatures (4 K in our cryostat) to prevent non-radiative recombination through impurities and thermal excitations [32], with optical access and often with electric contacts. It would also be preferable if the contacts allowed for easy attachment. Existing cryostats (Oxford Instruments Microstat He2) in the lab had optical access but lacked useful contacts so the contacts had to be built from scratch.

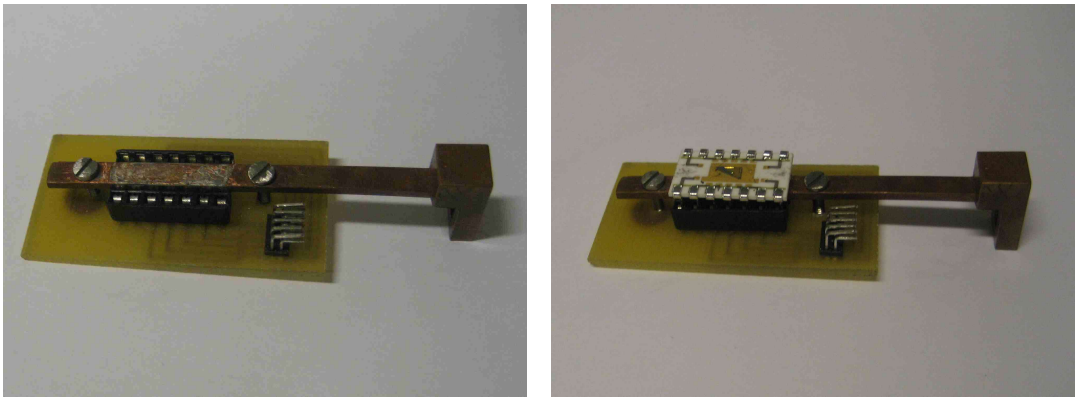

(a) Unmounted (b) Mounted R14 sample holder

Figure 14.: Coldfinger with electrical contacts instead of laboriously soldering on every individual lead. The R14 sample holder is easily snapped into place.

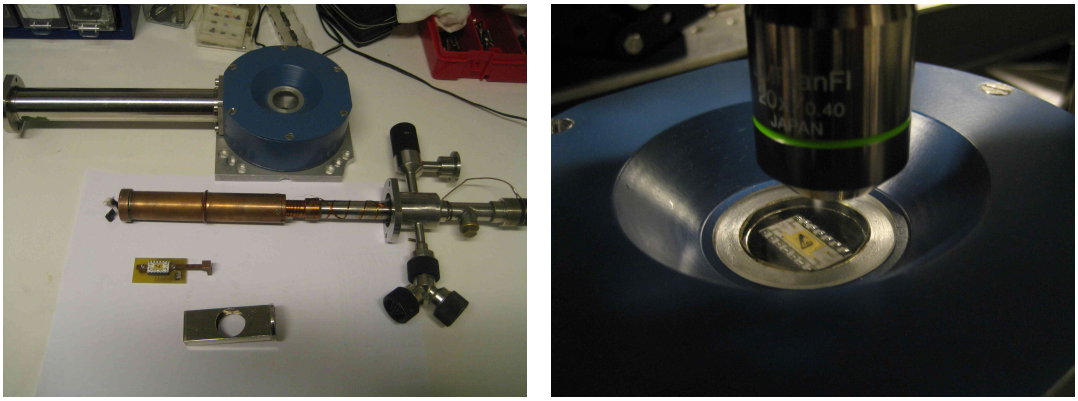

(a) Disassembled cryostat and shielding. (b) Sample in cryostat under microscope.

Figure 15.: He-Cryostat

Since most of the electrical measurements in the department are done by mounting the samples onto so called ”R14 sample holders” they were chosen as the base for the holder, the sample holder is shown in figure 14b. A low socket was chosen to fit into the shielding (25x35x10 mm) and a circuit was printed and etched onto a circuit board. Thin insulated copper wires served as contact and were gathered in a connector for easy detachment from the circuit board. The wires were left without a protective shell to reduce strain.

A cold finger of copper was modified so that the sample holder could straddle it when connected to the socket. The thermal contact was then through the cold finger, the sample holder, and the sample itself. To create a better thermal anchoring, Agar silver glue is meant to be used to glue the sample holder to the cold finger the same way the sample is glued to the R14. The completed coldfinger is shown in figure 14b.

With all the extra mass and surface area it might be harder to keep the temperature low, so an investigation was carried out to establish the temperature with the new cold finger.

A diode is incorporated into the cryostat but is situated near the cooling helium so it can not be used to measure on the finger itself. A new temperature sensor (Lakeshore DT-470-SD) was glued both directly to the cold finger and on the sample holder. It was found that even without the extra mass of the entire holder the finger itself never reached temperatures lower than 17 K. The added parts gave roughly 10 K higher temperature. So the average temperature when measuring is probably around 25-30 K. See figure 15 for an image of the assembled cryostat.

After using the sample holder in several measurements it has proven reliable despite the low temperatures that are far from the specifications for the individual components (plastic sockets, circuit board etc) and cycling the temperature from 20 K to 300 K on a regular basis.

However, some of the connecting wires have had to be repaired after repeated detaching of the sample holder. One solution to provide safer contacts could be to bridge the final distance with a thicker, more flexible wire. Another is to dedicate one cryostat to that setup to avoid detaching the cold finger.

It is necessary to be able to ground the connections between gate and substrate since the devices on the the sample are very sensitive to electric discharges. 50 Ω resistors were used to ground the sample when not in use. The results of neglecting to properly ground the sample is seen in figure 16.

2.4 OPTICS TABLE

The measurement setup used can be seen in figure 17. The sample is mounted on the cold finger in a liquid helium cryostat with a window for optical access. The cryostat itself is mounted on a translation stage.

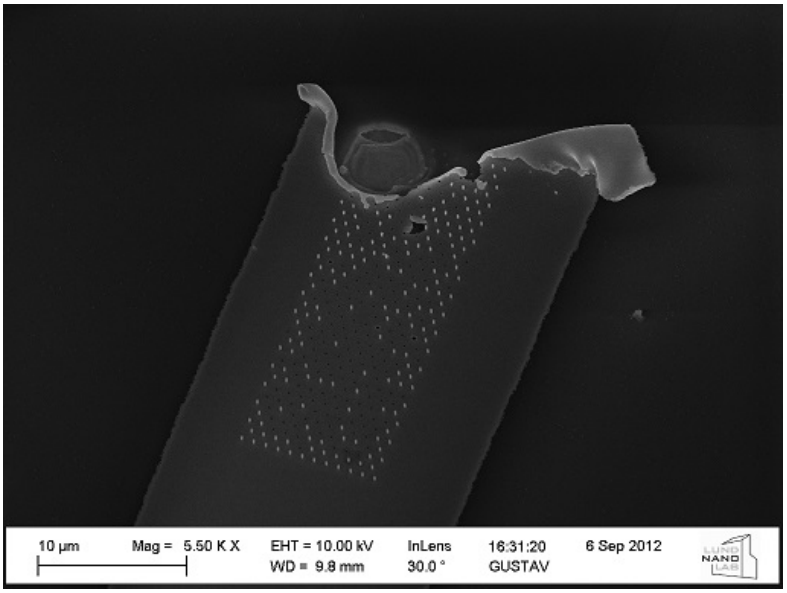

Figure 16.: A SEM image of an exploded array, likely when sample was not grounded properly when attached to voltage source. A majority of the NWs seem to have melted. (G. Nylund)

A tunable wavelength laser was aimed at the sample to create a big enough spot size to cover an entire array (roughly 75 μm diameter). The monochromator was occasionally used to remove unwanted wavelengths from the laser, it was the inserted before the polarizer. A microscope gathered the PL light and passed it into a diffraction spectrometer after filtering away the exciting laser light.

A grey filter with adjustable transparency was used to change the excitation intensity.

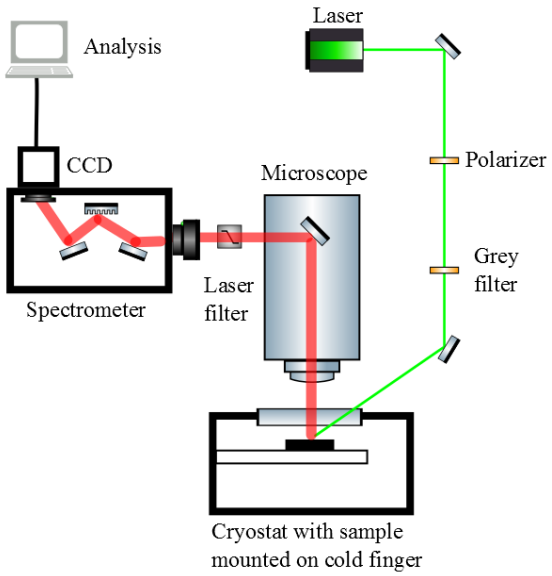

Figure 17.: Typical optics table setup, depending on experiment other components such a wave plate, monochromator and power meter were inserted into the beam line.

3

MEASUREMENTS

We wanted to investigate the properties of the wrap gated nanowires. A summary of the doping dependent measurements is found in table 2.

We expected to see n- and p-doped samples to respond to gate bias in the same way but with opposite sign and that thinner NWs should be strongly affected by gate bias.

What we observed was that surprisingly, thin NWs resisted effects from bias, I attribute this behaviour to the surface effects being relatively stronger at small scales and overtaking the effects of the gate bias. I don't have a good model for the p-doped samples not responding to bias other than to hazard a guess that they formed a Shottky diode contact.

This unfortunately hampered the original plan to study excitons and the study was shifted to how and why the different doping types affected the bias response.

In a typical measurement the samples where electrically bonded and put in the cryostat. The NWs were excited from the side with a red 750 nm (1.66 eV) 80 mW laser with a spot size of $\sim 75\mu$m giving an intensity of 450 W/cm^2. The high intensity was enough to cause state filling and could be attenuated with a gray filter.

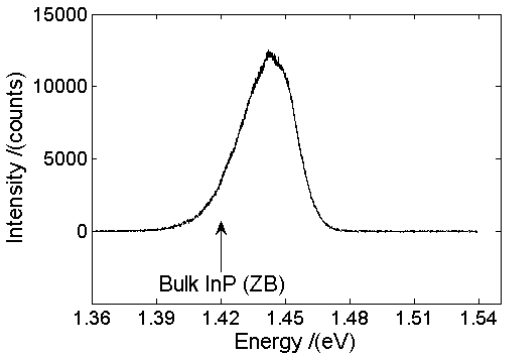

Figure 18.: Typical PL spectrum from an undoped InP NW array, the bandgap for bulk InP ZB is indicated.

In figure 18 we can see a typical PL spectrum from a 0.1 s exposure, a sharp peak above the bandgap without any features. The bandgap energy for bulk InP zincblende (ZB) is indicated for reference.

In many measurements we are interested in the total intensity of the peak to get an estimate of what the electron-hole population is. This is obtained by integrating over the peak and getting a single value.

Structure	Experiment	n-type	i-type	p-type
Ungated Arrays	PL visible?	Yes	Yes	Yes
	Diameter dependence?	weak	strong	strong
Gated Arrays	PL after deposited gate?	Yes	Yes	No!
	PL respond to gate bias?	Yes	Yes	No!
Single gated NWs	PL respond to gate bias?	Yes	Yes	weakly in one sample!
	Finestructure requires?	low intensity and applied bias	low intensity and applied bias	-

Table 2.: Summary of doping dependent results, notice that ITO gate suppressed PL in p-type NWs.

3.1 UNGATED NWS

3.1.1 *Photoluminescence radius dependence*

Arrays of nanowires with diameter from 40-70 nm were excited with a 750 nm laser. A collection of typical PL spectra from one measurement can be seen in figure 20c, each line corresponds to one NW diameter, the integrated intensity is seen in figure 21. p-doped and undoped NWs showed a linear increase in luminescence intensity with the diameter but extrapolating backwards there seems to be a threshold radius of 20 nm under which no PL occurs, the increase thus seems roughly linear but not proportional with NW radius. Extrapolating a a proportional increase should intersect the origin instead of the x-axis at 20 nm. n-doped Nws only had a very weak linear dependence, a 30 % increase compared to 2500 % for p-doped wires over 15 nm radius. I have chosen not to correct for NW volume since I'm not sure if the physics happen in the entire NW, just the surface or at some localized traps. The increase in volume is $\sim$ 300 % from the thinnest to thickest NWs but is not enough to explain the large increase in p-doped NWs, especially since both n- and p-doped NWs have the same dimensions. Even an assumption of a dead layer does not fit with the non quadratic increase one would assume in a first approximation where the PL intensity is only based on the NW volume and thus the number of electrons in the NW.

The strong nonproportional increase, starting at the threshold diameter 40 nm instead of 0 nm, is an indicator that it is not a simple volume effect.

In figure 19 I have modelled the charge carriers in an InP NW. When the radius is small the NW gets depleted unless it has a high doping. This would explain why the PL does not simply increase proportionally with NW volume in figure 21c. A first approximation of the number of charge carriers available ought to be that they scale with volume and thus would increase proportionally with volume. But this is shown not to be the case.

The behaviour of the charge carriers suddenly increasing at a diameter of 40 nm is reproduced in figure 22 where $D_{it} = 3 \cdot 10^{12}$ is chosen to fit the data.

It is a bit unfortunate that the lowest diameter chosen for the radius measurements was so close to the cut off diameter. The smallest diameter was chosen as it was the smallest possible to manufacture with that technique. Ideally it would have been reassuring to have thinner NWs to confirm that they also are depleted.

Also NWs seemed to "lose" the diameter dependence after adding and removing gate as is discussed below in section 3.1.2. It could be that all the n-doped samples had some faulty processing but it is unlikely since the gate processing was made at the same time for p-doped samples and they showed no signs of problems.

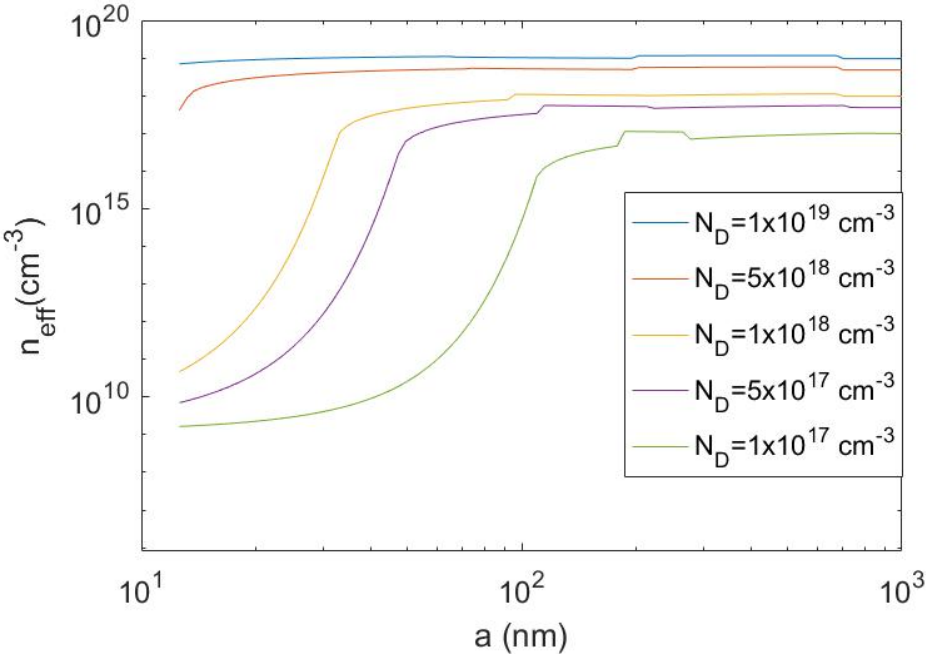

Figure 19.: Modeled charge carriers at different doping levels and radius in InP NW. D_{it} was 10^{13} $cm^{-2}eV^{-1}$. Thin NWs are depleted due to surface effects unless heavily doped.

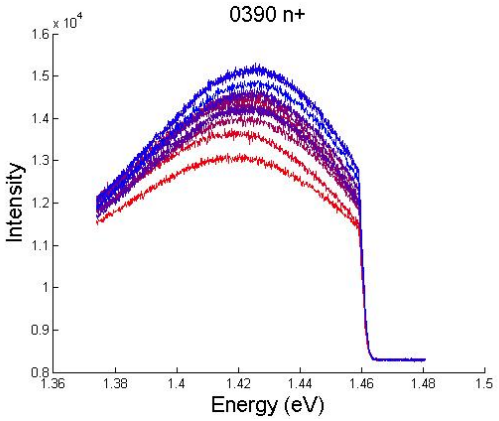

(a) Spectrum from n-doped arrays with different diameters, almost nothing happens.

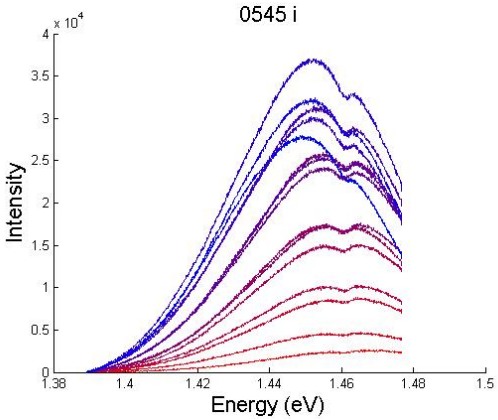

(b) Spectrum from undoped arrays with different diameters. The small dip at 1.46 eV is from an uncalibrated effect in the monochromator.

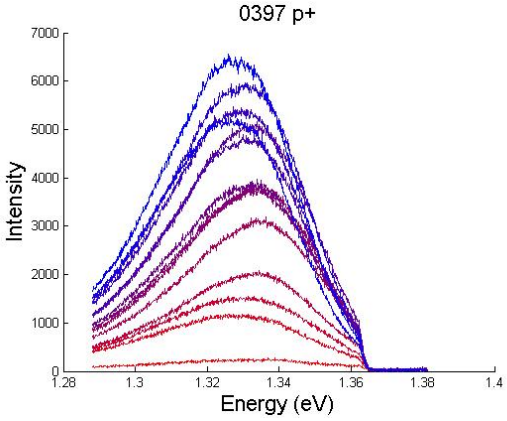

(c) Spectrum from p-doped arrays with different diameters.

Figure 20.: Arrays with different diameters and doping. NW diameter increase from 40 nm (red curve) to 70 nm (blue curve).

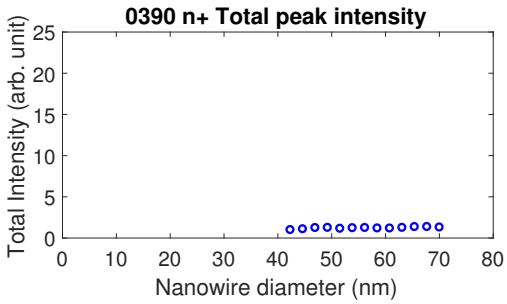

(a) n-doped

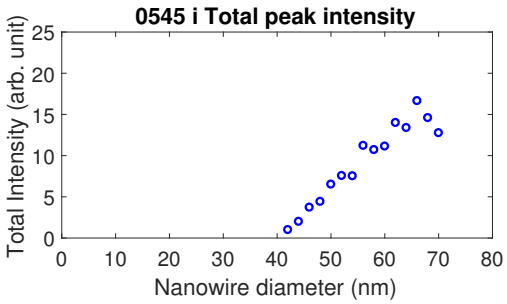

(b) undoped

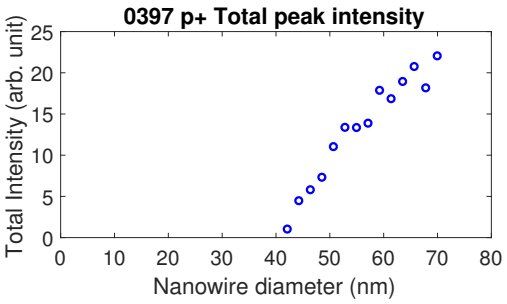

(c) p-doped

Figure 21.: Integrated intensity from figure 20, the lowest intensity within each series is normalized to 1. n-doped show only a small increase in intensity with diameter but undoped and p-doped NWs increase roughly linearly from non-zero radius. At each diameter the NWs are of equal length but the intensity is not corrected for volume.

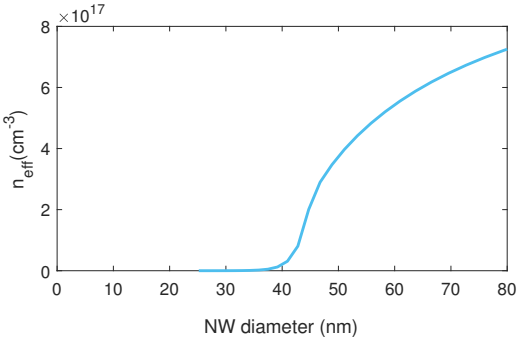

(a) Modelled electron concentration n_{eff}.

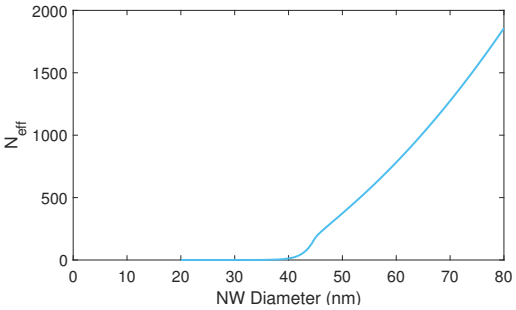

(b) Modelled total population of electrons N_{eff} in the NW, $N_{eff} = n_{eff} \cdot$ volume. Compare with figure 21c. The sudden increase in population at some diameter is described by the model but not the different behaviour of the n-doped sample.

Figure 22.: Modeled charge carriers in InP NW when $N_D = 10^{18}$ cm^{-3} and $D_{it} = 3 \cdot 10^{12}$ cm^{-2}eV^{-1}.

3.1.2 *Removed ITO*

We were surprised to find that the photoluminescence disappeared after adding the gate to the p-doped NWs since they had showed a strong diameter dependence without the ITO gate. To establish if it was the ITO or some other phenomena that impacted the PL the gate was removed with acid etching. In theory the NWs should revert back to their ungated form but considerable differences in the spectrum where left. The diameter dependence seemed to disappear (see figure 23), notice however that some devices have returned to strong luminescent intensity compared to the devices that had decreased PL. To me this indicates that the etching was partly unsuccessful in the devices with decreased PL. Effects of etching on InP surface trap density has been reported in [33].

If the decrease in intensity is attributed to ITO residues we can explain the drop by increased surface trap density (D_{it}). The modelling suggests that even the thickest NWs will be depleted of charge carriers and PL intensity when D_{it} increases to about 1 % of the surface atom density as seen in figure 24.

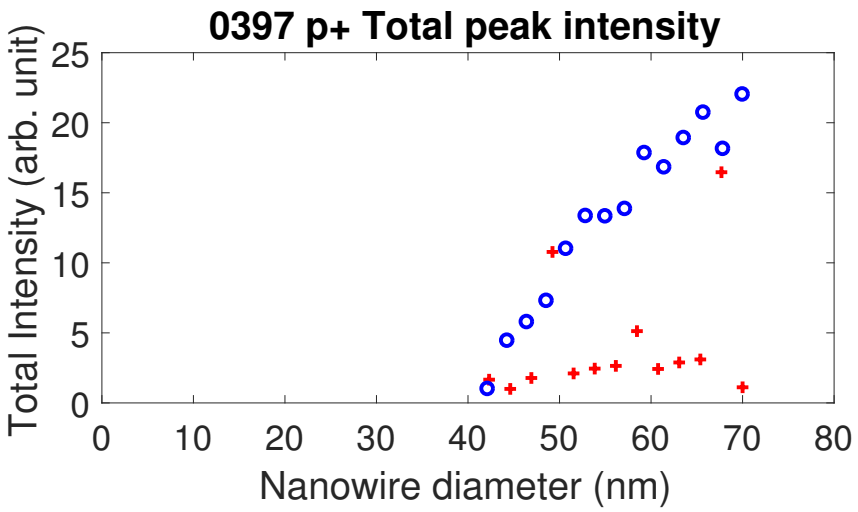

Figure 23.: Blue "o" is PL intensity before added gate. Red "+" is PL intensity after the gate has been added and the removed with etching. Notice that some devices seems to be fully restored by the etching. Notice that the lowered intensity is more comparable to the n-doped in figure 21a.

3.2 GATED NANOWIRES

3.2.1 *Photoluminescence gate dependence*

Only n-doped and intrinsic NW arrays showed any response to gate bias (both positive and negative). Bias dependent PL spectra can be seen in figure 25. The integrated intensity is seen in figure 26 where we can see that the total emission intensity was constant from negative bias until a threshold where it increased until a new cutoff where it seemed to level out. Increasing the bias more than this first causes the leakage current to increase sharply and then a catastrophic breakthrough in the gate oxide, the corresponding drop in luminescence can be seen around 7 V in figure 26. This is consistent with being in the accumulation regime of a MOS-capacitor.

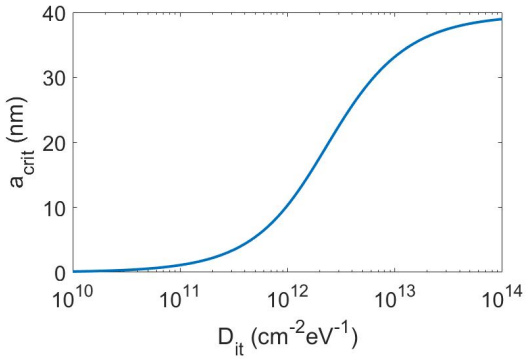

Figure 24.: Critical radius (a_{crit}) for completely depleted nanowire depending on interface states (D_{it}). Doping is $N_D = 10^{18} cm^{-3}$. The concentration of surface atoms in InP is $10^{15} cm^{-2}$ so about 1 % made into interface traps would be enough to cause depletion in our NWs. This figure is likely critical in understanding why the NW PL is so radius sensitive.

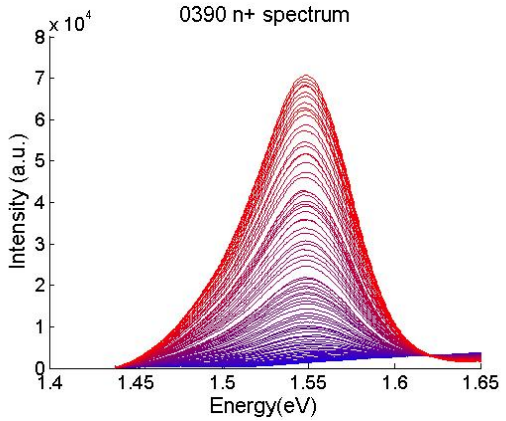

Figure 25.: PL for different gate bias, from blue, -2 V, to red, 7 V.

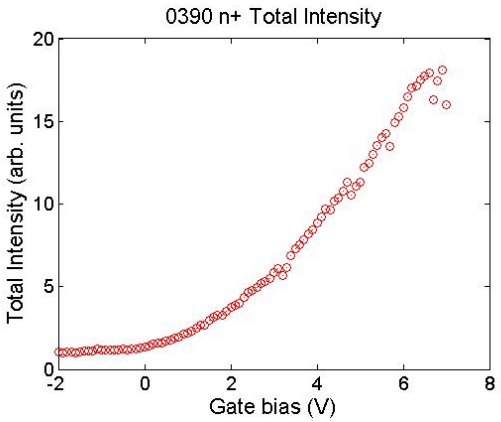

Figure 26.: Integrated PL for biased n-doped NWs, the linear increase from a certain forward bias is consistent with the behaviour charge carriers in the accumulation regime of a MOS-capacitor. The drop in luminescence at 7 V corresponds to the beginning of breakthrough in the gate oxide.

p-doped arrays did not show any response to gate bias but single NWs showed some, see below. The wrap gate did also seem to suppress the p-doped luminescence, it had been visible without a gate, but after the gate was processed the signal disappeared. The gate possibly facilitates non-radiative recombination or maybe "pushes" the holes or electrons away from the NW. This was not observed in the n-type NWs.

However, in later experiments with a single lateral NW there was a small response seen in figure 27. The measurement was noisy but it seems as if the p-doped sample behaves similar to n-doped, but increasing after a threshold with negative bias instead. Again consistent with accumulation but for a p-doped MOS-capacitor.

This was the expected result from the start, but more experiments needs to be made since we only saw the response in a single device.

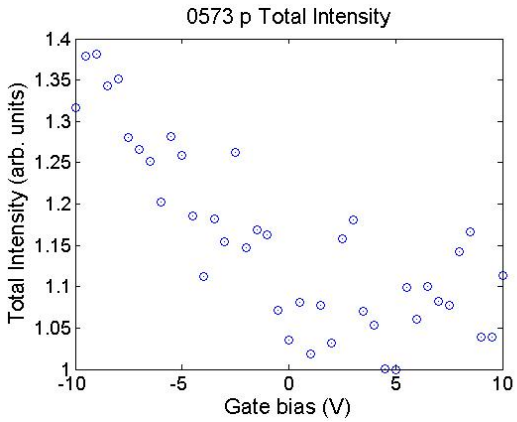

Figure 27.: Integrated PL for biased p-doped single NW, the only p-doped device to show any effect of gate bias.

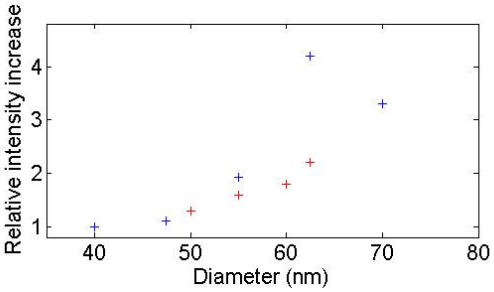

h

Figure 28.: Relative intensity increase when bias is increased from 0 to 3 V at different diameters of n-doped NW arrays. The red and blue data points are from two separate measurements. We can see that at 40 nm diameter there is no effect of gate bias but it increases quickly with diameter.

3.2.2 *Photoluminescence radius dependence on gate*

Sweeping the gate bias of n-doped NW arrays from low to high (0 to 3 V) showed a higher relative increase in luminescence at bigger radius. This can be seen in figure 28 where we maybe see a more than linear increase but it is hard to tell with few data points. Notice however that since it is relative increase in intensity that is plotted we go from almost no change at the 20 nm radius to more than 4 times the luminescence at 35 nm. This is also interesting since the n-doped NWs showed only a weak radius dependence in figure 21a before depositing the gate. The physics behind gate induced PL seems more strongly affected by different radius than just the laser generated PL where the increase was small in n-type NWs. Originally I expected the thin NW to be the most affected by gate bias since while the total capacitance is smaller (essentially less surface area) the surface to volume ratio is larger so there should be fewer charges to affect ($Capacitance/volume \propto 1/NWradius$).

3.2.2.1 *Results from simulations*

The simulation from section 1.9 is illustrated in figure 29 shows that thin NWs might already be so depleted from the effects of D_{it} that their energy bands are unaffected by bias. This could explain the results in figure 28 where thin NWs are less affected by gate bias.

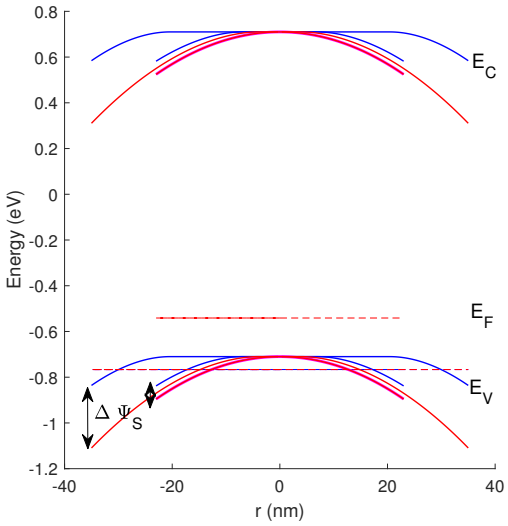

Figure 29.: Band structure in p-doped NW with radius $r = 22$ and 35 nm represented by the widths of the potentials. Red is a gate bias of 0 V and blue is a gate bias of -3 V. The surface potential $\Delta\Psi_s$ is less affected in the thin NW since it is almost depleted already. The narrow and wide lines represent the E_F for the thin and thick radius respectively.

3.2.3 *Uneven PL from arrays*

The arrays did not always luminesce with an even distribution, more along the sides or in small islands as is seen in figure 30. Several reasons are possible but it should not be due to gate oxide thickness variance since it is highly controlled with the atomic layer deposition (ALD) technique. Maybe broken NWs are still standing or the gate could perhaps bond differently with the NWs. It is unlikely leaking light from the substrate since it had a different spectrum compared to naked substrate and responded to gate bias.

Even though commercial products would likely need to use arrays for scaling, for investigative physics research it will probably be best to focus on single NWs. We then get a better signal to noise ratio by looking at single NWs if the effect we are looking for is only present in some of the thousands of NWs in the array. We can be sure that

the PL is from the NW and not from substrate and be surer that the bias is placed evenly around the NW.

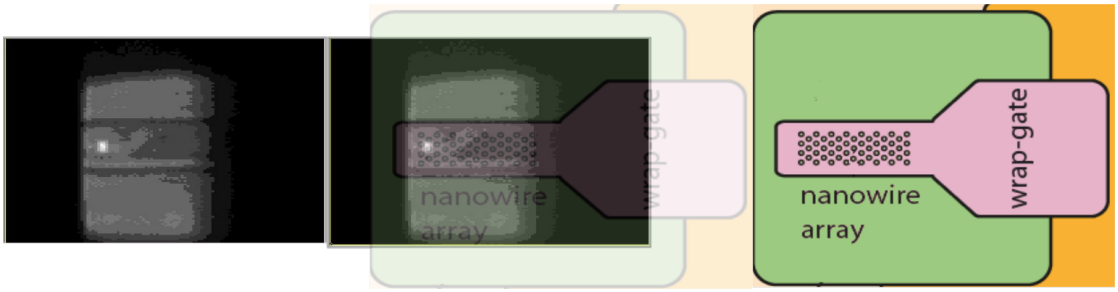

Figure 30.: Image of an array with both laser and white light from the microscope (captured with the monochromator) with superimposed schematic of the array. The array covers the wide horizontal band. The array is not luminescing evenly and only from one corner.

3.3 SINGLE NWS

The p-doped arrays did not show any gate response and their PL peak disappeared after adding the ITO wrap gate, so to further investigate and see if the results were due to some physical phenomena or just fabrication error the measurements continued with single lateral NWs instead. By only looking at a single NW at a time we can be more sure that the bias is placed at the right place and not lose any interesting PL signal in forest of the others in the array. We can also inspect the each device closely in a SEM to look for obvious defects. This also lets us confirm that any results are from the NWs and not light leaking up from the bulk substrate since the substrate is covered with a lightblocking film of gold.

A huge issue with the single NW experiments is that they had unknown and possibly different radius, a factor that was shown in figure 28 to highly impact gate dependence.

3.3.1 *Photoluminescence gate bias intensity dependence*

PL is measured at different intensities while sweeping the gate bias. An emerging fine structure could be seen at low intensities and manipulated in intensity with the gate bias in figure 31.

The voltage sweep in the measurements was done in 10 s intervals. It started at 0 V, was dialed back to negative bias and then increased until leakage current started to increase.

h

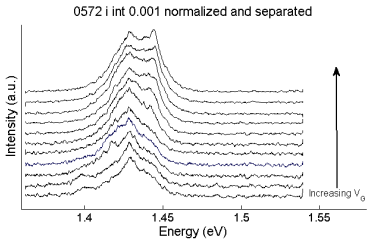

(a) Undoped NW at low intensity

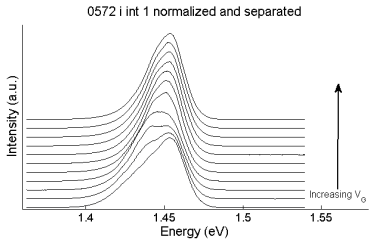

(b) Undoped NW at high intensity

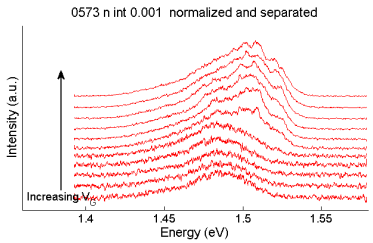

(c) n-doped NW at low intensity

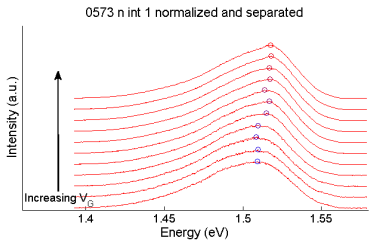

(d) n-doped NW at high intensity

Figure 31.: Single NWs at different intensities and bias. At low intensities there is some kind of fine structure that changes with gate bias.

The total intensity of the peak responded quite unexpectedly in figure 32- the spectrum required a lower threshold bias to increase the PL intensity under a high exciting intensity compared to a low exciting intensity, (0.001 of the high exciting intensity). Hysteresis effects where water molecules on the surface of the NWs store charge have been discussed in [24] and could be an explanation for the moving threshold bias in figure 32 even though care was taken to be systematic. Here the experiment could be repeated with a different order of applying the gate bias to rule out hysteresis effects.

A very loose speculation is that there are defects with non-radiative recombination (also called Schokley-Read-Hall (SRH) recombination (see section 1.7) [34]) or wells that need to be filled before the extra charge carriers attracted by the bias can spread out to the regions of the NW where radiative recombination is more likely. We do also see a more than proportional increase in PL with the exciting intensity in figure 36 giving support to the speculation. I expect an increase in a from equation (14) in the regime after the defects saturate, the population would then have a larger fraction of radiative transitions and thus the PL intensity would scale faster with increasing laser intensity. At the defects the charge carriers will have to wait in line to recombine whereas band to band transitions only get faster the more charge carriers there are.

This could also explain the fine structure seen at low intensities in figure 31c and 31a. At high excitation power the defect recombination will saturate and be lost among the band to band transitions that scales faster with laser intensityr.

h

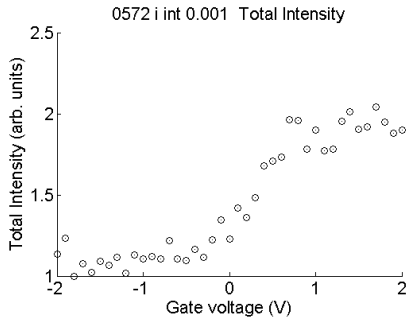

(a) Integrated PL for undoped NW at low intensity, threshold bias at -0.25 V.

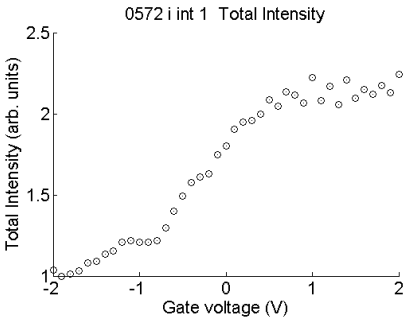

(b) Integrated PL for undoped NW at high intensity, threshold bias at -0.75 V.

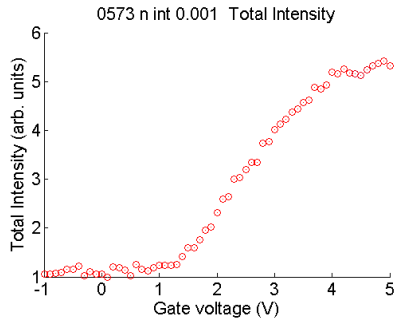

(c) Integrated PL for n-doped NW at low intensity, threshold bias at 1.5 V.

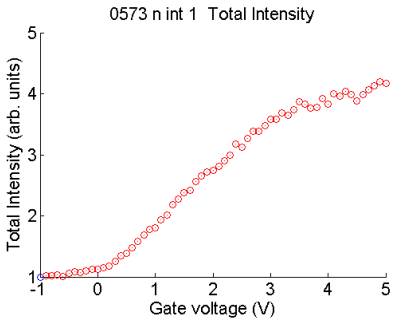

(d) Integrated PL for n-doped NW at high intensity, threshold bias at 0 V.

Figure 32.: Integrated PL at different intensities and bias. The threshold bias seems to be lower at higher intensities.

Type	minority m_e (m_0)	Peak shift (meV/decade)	relative $1/m_e$	relative Peak shift
p+	0.077	37	1	1
undoped	0.068*	12**	1.13	0.32
n+	0.6	4.4	0.13	0.12

Table 3.: Effects of effective mass. Energy bands fill with $E(k) = \frac{\hbar^2 k^2}{2m_e}$ and for heavily doped materials the peak shift should be proportional to $1/m_e$ of the minority charge carrier. The doped samples behave as expected but the undoped measurements contradict the model. *$1/m_u = 1/m_p + 1/m_n \Rightarrow m_u = 0.068$ **Extrapolated, see figure 33c.

It has been proposed that the peaks are from quantum wells formed by stacking faults between zincblende and wurtzite[35] regions in the NW. In my opinion there are arguments against that explanation since the peaks are separated about 1 order of magnitude more than what is suggested by a simple 1-D QM-well model.

3.3.2 *Peak shift intensity dependence with doping*

With increased excitation intensity the peak energy seems to blueshift linearly on a semilogaritmic plot for high intensities as is shown in figure 34 and 35. The shift is stronger for p-doped compared to n-doped NWs, the difference seems to be inversely proportional to the difference in effective mass of the minority charge carriers (see table 3). A model for this is discussed in section 1.5 where the speed of the blueshift should be inversely proportional to the effective mass of the minority charge carriers when the bands are filled with charge carriers due to high exciting intensity.

How the peak energy moves when the excitation power is increased is non-trivial, increased population leads to increased emission and finally some new steady state.

Excited charge carriers in bulk InP are also known to have long lifetimes (1-100 ns) even when doped [2] [36] [37] so they have a relatively long time to fill the band.

A strong indicator that the effective mass model is flawed however is that the undoped measurements contradict this model. They should blueshift even faster (from a thin peak) than p-doped samples (wide peak). Also the n-doped PL intensity doesn't increase as neatly with excitation power as the p-doped.

Because of experimental problems p and n-doped NWs was measured with excitation laser focused through the microscope whereas undoped was measured with laser from the side, giving a larger spot size and lower intensity. It is possible that n- and p-doped NWs entered another saturation regime. This is also indicated by figure 36 where the undoped intensity seemed to increase in two regimes.

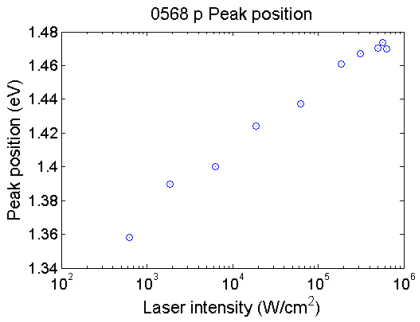

(a) Peak energy shift for p-doped NW.

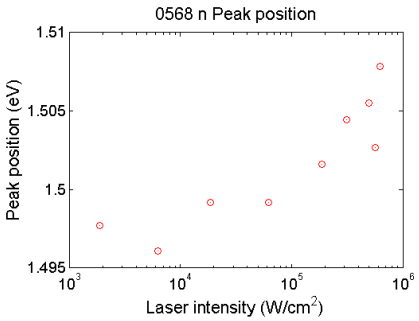

(b) Peak energy shift for n-doped NW.

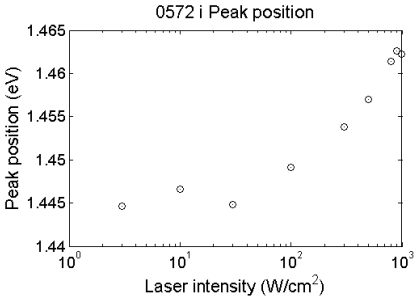

(c) Peak energy shift for undoped NW. Notice the lower exciting intensity used, extrapolated to the higher intensity gives a 50 meV peak shift.

Figure 33.: Intensity dependent peak energy for lateral NWs.

The relative intensities used are reliable but it is hard to estimate the absolute intensity when the beam profile is focused at an angle (even though care was taken to be consistent). It has been reported in [38] that a thin GaAs film was heated from 10 K to 100 K at exciting power $120 \cdot 10^3$ W/cm2 (in the same ballpark as reported in my experiments). A very similar setup to mine was used to estimate the electron temperature in an n-InP NW sample to 144 K [21]. This will certainly shift the electron population up by $\Delta kT/2 = 4$ meV (see equation (1)) but the bandgap E_g decreases 20 meV with temperature according to equation (2) so these effects should roughly cancel out and if anything contribute to a redshift rather than a blueshift. In my experiments I haven't seriously studied the effects of the time the pump laser is active but I also haven't noticed any differences from short exposures. So any heating is probably instantaneous.

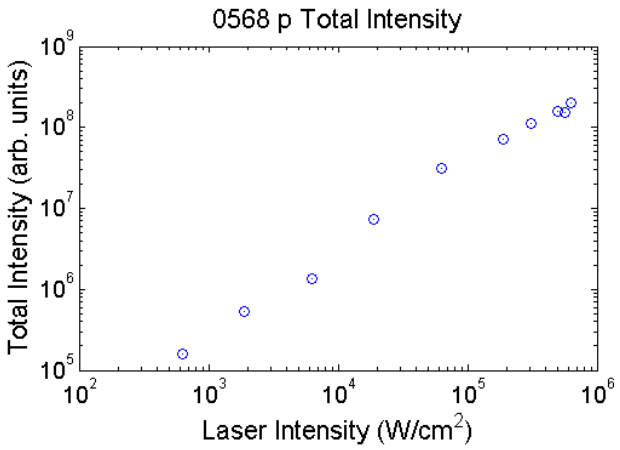

Figure 34.: PL intensity vs excitation intensity for p-doped NWs. Here $I \propto E_{exc}^{0.8}$

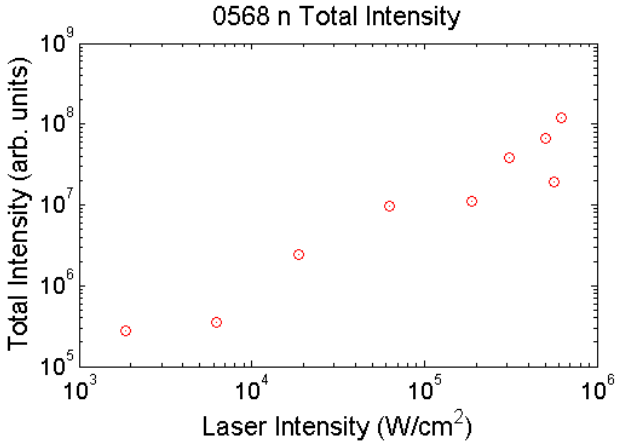

Figure 35.: PL intensity vs excitation intensity for n-doped NWs.

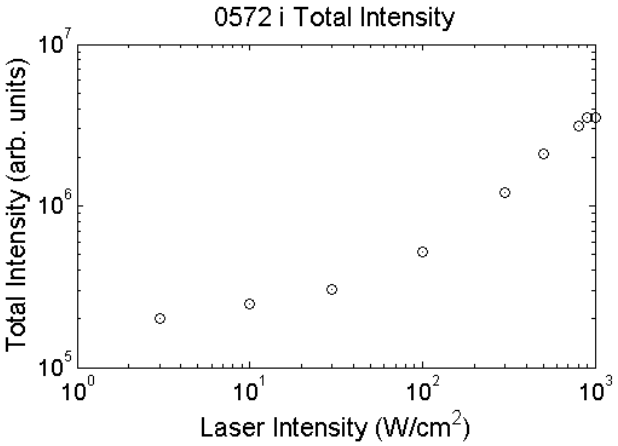

Figure 36.: PL intensity vs excitation intensity for undoped NWs. Notice that the intensity used is lower than in n and p-doped.

3.3.3 *ITO and laser wavelength*

Normally an exciting wavelength of 750 nm was used, but when 532 nm was used the PL from the NWs disappeared. A broad band of luminescence appeared in figure 37 that seems to be luminescence from the ITO gate. ITO absorption in thin films is highly dependent on interference [39], meaning that from sample to sample there can be a big difference. Interfaces with other materials can also affect the transmission as seen in figure 12.

The green laser is close to the absorption edge of ITO so if it is changed a little it can give drastic effects on the transmittance. Red lasers were used to avoid this behavior.

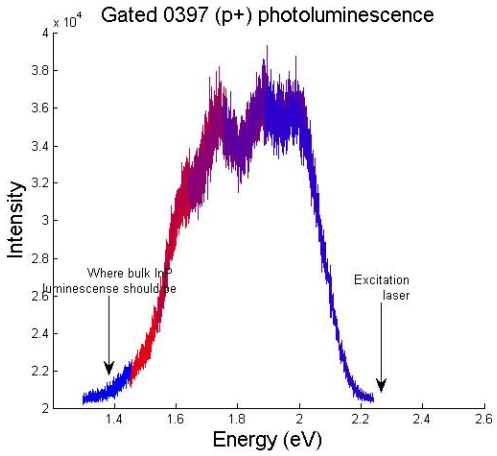

Figure 37.: PL taken with green excitation laser, the ITO seems to luminesce strongly.

4

CONCLUSIONS AND OUTLOOK

The motivation for the project was to find a way to separate excitons in InP NWs and observe them through a transparent ITO wrap gate. Or at least do a pre-study for a later project.

It turns out that while the ITO wrap gate is mostly transparent it also directly affected the photoluminescence in the NWs, especially in p-doped NWs. No cause was established but if the ITO increased the density of interface states as has been reported by others, simulations show that the concentration of free charge carriers goes down dramatically due to depletion in the entire NW.

The R14 sample holder socket straddling a cold finger greatly simplified testing several devices and achieved temperatures of 25-30 K.

Different exciting intensity dependent peak shifts were seen in n- and p-doped NWs. A model based on the effective masses of the minority charge carriers during state filling was proposed to explain the peak shift but with inconclusive results.

p-doped NW PL only showed signs of being affected by the wrap gate in a single device, otherwise behaving as if suppressed by the gate. This possibly limits the use in future devices but warrants deeper investigation in as to why .

Both undoped and p-doped NWs seemed to increase their PL linearly with diameter from a "dead diameter" of roughly 20-30 nm. This was attributed to the NW being depleted by interface traps. For ungated n-doped NWs the PL intensity was almost independent of NW diameter but the effect of gate bias proved to be diameter dependent with increasing effects of gate bias at wider diameters. I could not explain why the n-doped NW seem unaffected by diameter but the un- and p-doped NWs are.

4.0.4 *Outlook*

If the ITO wrap gate does increase the density of interface states that effect could be reduced. The surface might be passivated by growing a high bandgap insulating shell made of for example PO_x around the NW core before adding the gate [40]. The transient tail from the electron states in the metal-like ITO might not reach through a thicker oxide to create metal induced gap states. In essence sacrificing some electrostatic capacitance to reduce unwanted nanoscale surface effects.

Further research would be needed to determine how the ITO wrap gate functions differently with the p- and n-doped samples.

I would also like to test the state filling with another direct bandgap III-V material NW such as GaAs to see if the peak energy also shifts inversely proportional to the minority carrier effective mass. I would expect the n-doped NWs to blueshift due to state filling at $0.063m_0/0.51m_0$=0.123 the speed of p-doped NWs.

One of the ways to identify bandbending was initially thought to be the changed recombination rate when electrons and holes are spatially separated in the core and surface. This proved difficult to observe without time resolved spectroscopy, as otherwise we should eventually reach a steady state from the optical pumping regardless of recombination rate. In time resolved spectroscopy the pump laser is not active during the actual measurement of fluorescence, so that we can see the transient behaviour of the undisturbed system, this should clarify if the changes in peak energy position where from band bending or some other effect such as state filling.

4.0.5 *Closing words*

This thesis set out to find spatially separated excitons and while that goal quickly faded into obscurity I managed to pinpoint some challenges with the intended experimental design. I hope the next one to attempt this carefully examines the surface properties of their chosen materials before starting the fabrication phase. Good hunting!

⊙

A

APPENDIX

In figure 38 we see the band diagram that we want to model.

Start in Poisson's equation (15) in cylindrical symmetry with r as radial distance from center

$$\frac{\partial^2 \psi}{\partial r^2} + \frac{1}{r}\frac{\partial \psi}{\partial r} = -\frac{\rho}{\epsilon} \tag{15}$$

where ψ is the electric potential, ρ is the net bulk charge density, and ϵ the permittivity of InP. This has the solution,

$$\psi(r) = -\frac{\rho}{4\epsilon} r^2 + C_1 \ln r + C_2 \tag{16}$$

where C_1 and C_2 are constants[41].

The distance from the NW center that is quasi-neutral (corresponding to normal bulk conditions) is called r_q. A smooth transition from the center to depleted edge requires the following boundary conditions for the potential at the radius of the quasi-neutral core r_q,

$$\psi(r_q) = \psi_0 \tag{17}$$

and

$$\left.\frac{d\psi(r)}{dr}\right|_{r=r_q=0} \tag{18}$$

In the depleted region of an n-type NW the ionized donors (N_D) vastly outnumber the electrons $n(r)$, holes $p(r)$ and acceptors N_A ($N_D \gg n \gg p, N_A$). Since the ionized dopants and their charge carriers cancel out in the quasi neutral core the charge density ρ in the NW is

$$\rho = \begin{cases} 0 & \text{for } 0 < r < r_q \\ qN_D \equiv \rho_g & \text{for } r_q < r < a, \end{cases} \tag{19}$$

where a is the radius of the NW. The boundary conditions (18) and (17) together with the charge density (19) gives the solution for the potential $\psi(r)$ as

$$\psi(r) = \begin{cases} \psi_0 & \text{for } 0 < r < r_q \\ \psi_0 + \frac{\rho r_q^2}{2\epsilon}\left[-\frac{r^2}{2r_q^2} + \ln\frac{r}{r_q} + \frac{1}{2}\right] & \text{for } r_q < r < a \end{cases} \tag{20}$$

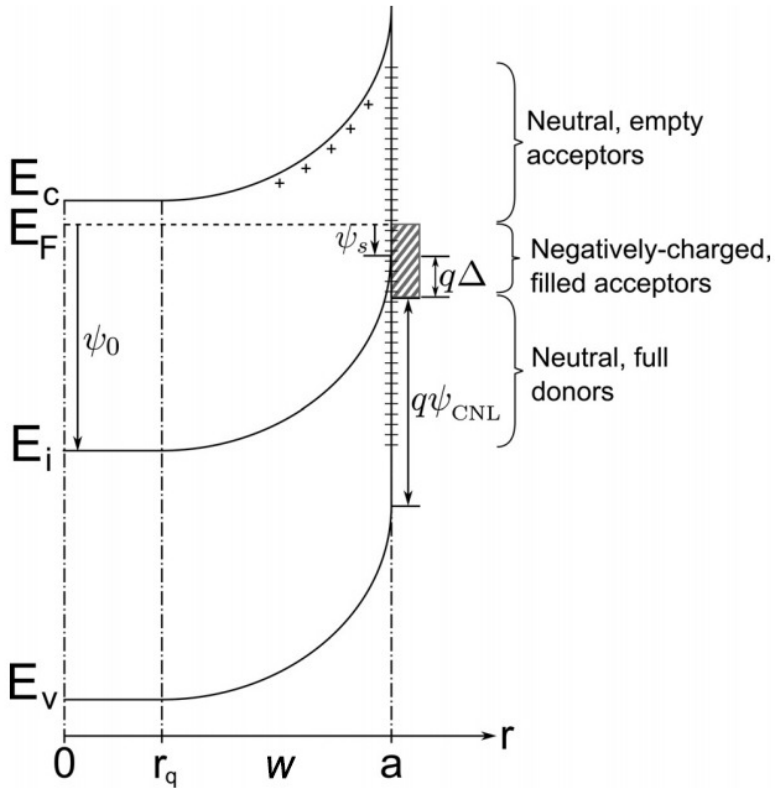

Figure 38.: Band diagram along the cross section of a NW. The interface states D_{it} are visualized as acceptors and donors at the radius a. Since the charge neutral level (CNL) is below the band midpoint E_i the interface states act as negatively charged filled acceptors and cause a charge $q\Delta$ that pins the band closer to the CNL. (Image by Chia et al with an added w to indicate the depletion depth)

.

To find the potential at the NW center ψ_0 we need to find the Fermi-level E_F. The NW can be highly doped and therefore the usual Boltzmann approximation is not used here, instead the full Fermi-Dirac integral is used to find the Fermi-level position.

The electron concentration is given by

$$n(r) = \frac{2}{\sqrt{\pi}} N_C F_{1/2}(\eta_F) \tag{21}$$

where $F_{1/2}(\eta)$ is the Fermi-Dirac Integral given by

$$F_{1/2}(\eta) = \int_0^\infty \frac{x^{1/2}}{\exp(x-\eta)+1} dx \tag{22}$$

and η_F is a quantity defined below describing the relative sizes of ionization energy of donors and the thermal energy

$$\eta_F = \frac{E_F - E_C}{kT} = \frac{q\psi(r) - E_g/2}{kT} \tag{23}$$

where N_C is the effective density of states in the conduction band, E_g the energy bandgap, k the Boltzmann constant and T the temperature.

Assuming complete ionization of an n-type NW lets us substitute ($n = N_D$) in Eq. (21). In the center of the NW we get

$$\eta_{F0}(\psi_0) = \left.\frac{E_F - E_C}{kT}\right|_{\text{centre}} = \frac{q\psi_0 - E_g/2}{kT} \tag{24}$$

where η_{F0} is the value of η_F in the center.

Substitute Eq. (24) into Eq. (22) and solve it numerically to find ψ_0.

That only leaves finding r_q (related to the depletion width $w = a - r_q$).

This time we look at the surface of the NW, specifically Eq. (20) with surface potentential $\psi_s \equiv \psi(r = a)$ together with surface charges and charge neutrality. As discussed in section 1.6 the interface traps D_{it} will also add charges to consider.

A variable Δ is defined as $\Delta = \frac{E_g}{2q} - \psi_{CNL}$.

The charge neutrality level (CNL) used was $\psi_{CNL} = 0.9$ V . This is for the crystal direction { 110 }[42]. Our NWs are grown in the { 111} direction [28] but their side facets are of unknown orientation casting some doubt on the used value for the CNL.

The surface charge Q_{it} is given by

$$Q_{it} = -q \int_{E_i - q\Delta}^{E_i + q\psi_s} D_{it} dE \tag{25}$$

and assuming a uniform D_{it} between $E_i - q\Delta$ and $E_i + q\psi_s$ this simplifies to

$$Q_{it} = -q^2 D_{it}(\psi_s + \Delta) \tag{26}$$

Charge neutrality states that the sum of all bulk and surface charges in the system is zero, here I will also expand the work in [26] and add the charges Q_m from a gate bias V_{ox} in accumulation regime.

$$Q_m = V_{ox} C_{ox} \tag{27}$$

where C_{ox} is the capacitance of the gate oxide.

$$\pi(a^2 - r_q^2)\rho_g + 2\pi a(Q_{it} + Q_m) \tag{28}$$

And we arrive at a transcendental equation in r_q

$$\frac{(a^2 - r_q^2)\rho + aQ_m}{2aq^2 D_{it}} - \Delta = \frac{\rho_g r_q^2}{2\epsilon}(-\frac{a^2}{2r_q^2} + \ln\frac{a}{r_q} + 1/2) + \psi_0 \tag{29}$$

.

This can be solved numerically, but for some values of D_{it} and N_D there exists a critical radius a_{crit}, for which the NW is fully depleted ($r_q = 0$).

This gives two cases for r_q: in the partially depleted NW where $a > a_{crit}$, r_q is given by Eq (29). When $a < a_{crit}$ and the NW is fully depleted then $r_q = 0$.

A similar approach to find the potential $\psi(r)$ in the partially depleted case is taken in the fully depleted regime as well. It gives us the following expression

$$\psi(r) = \psi_0 - \frac{\rho}{4\epsilon} r^2 \text{for } 0 < r < a \tag{30}$$

.

Here the potential in the middle of the NW ψ_0 is given by

$$\psi_0 = \frac{a\rho_g + Q_m}{2q^2 D_{it}} - \Delta + \frac{\rho_g}{4\epsilon} a^2 \tag{31}$$

The potential is now found in both the partially and fully depleted regime given values of D_{it}, a, and N_D.

The average carrier concentration can be found by integrating $p(r)$ and $n(r)$ across the NW radius.

$$n_{eff} = \frac{1}{\pi a^2} \int_0^a n(r) 2\pi r dr \tag{32}$$

This implemented solution is used in section 3 where the results from the measurements are discussed as an attempt to explain the behavior of the NWs.

BIBLIOGRAPHY

[1]M. de la Mata, C. Magén, P. Caroff, and J. Arbiol, "Atomic scale strain relaxation in axial semiconductor iii–v nanowire heterostructures", Nano letters **14**, 6614–6620 (2014).

[2]H. J. Joyce, J. Wong-Leung, C.-K. Yong, C. J. Docherty, S. Paiman, Q. Gao, H. H. Tan, C. Jagadish, J. Lloyd-Hughes, L. M. Herz, et al., "Ultralow surface recombination velocity in inp nanowires probed by terahertz spectroscopy", Nano letters **12**, 5325–5330 (2012).

[3]W. Walukiewicz, J. Lagowski, L. Jastrzebski, P. Rava, M. Lichtensteiger, C. Gatos, and H. Gatos, "Electron mobility and free-carrier absorption in inp; determination of the compensation ratio", Journal of Applied Physics **51**, 2659–2668 (1980).

[4]S. Tian, Z. Wei, Y. Li, H. Zhao, X. Fang, J. Tang, D. Fang, L. Sun, G. Liu, B. Yao, et al., "Surface state and optical property of sulfur passivated inp", Materials Science in Semiconductor Processing **17**, 33–37 (2014).

[5]W. Liang, "Excitons", Physics Education **5**, 226 (1970).

[6]F. Glas, "Critical dimensions for the plastic relaxation of strained axial heterostructures in free-standing nanowires", Physical Review B **74**, 121302 (2006).

[7]L. Rui-Bin and Z. Bing-Suo, "Lasing behaviour from the condensation of polaronic excitons in a zno nanowire", Chinese Physics B **20**, 047104 (2011).

[8]E. Biolatti, R. C. Iotti, P. Zanardi, and F. Rossi, "Quantum information processing with semiconductor macroatoms", Physical review letters **85**, 5647 (2000).

[9]H. Takato, K. Sunouchi, N. Okabe, A. Nitayama, K. Hieda, F. Horiguchi, and F. Masuoka, "High performance cmos surrounding gate transistor (sgt) for ultra high density lsis", in Technical digest., international electron devices meeting (IEEE, 1988), pp. 222–225.

[10]C. Kittel, P. McEuen, and P. McEuen, *Introduction to solid state physics*, Vol. 8 (Wiley New York, 1996).

[11]M. S. Shur, *Handbook series on semiconductor parameters*, Vol. 1 (World Scientific, 1996).

[12]S. Perkowitz, *Optical characterization of semiconductors: infrared, raman, and photoluminescence spectroscopy*, Vol. 14 (Elsevier, 2012).

[13]J. Noffsinger, E. Kioupakis, C. G. Van de Walle, S. G. Louie, and M. L. Cohen, "Phonon-assisted optical absorption in silicon from first principles", Physical review letters **108**, 167402 (2012).

[14]S. M. Sze and K. K. Ng, *Physics of semiconductor devices* (John wiley & sons, 2006).

[15]D. Fitzgerald and A. Grove, "Surface recombination in semiconductors", Surface Science **9**, 347–369 (1968).

[16]B. E. Saleh and M. C. Teich, *Fundamentals of photonics* (John Wiley & Sons, 2019).

[17]J. H. Davies, *The physics of low-dimensional semiconductors: an introduction* (Cambridge university press, 1998).

[18]J. A. Del Alamo, "The high-electron mobility transistor at 30: impressive accomplishments and exciting prospects", (2011).

[19]C. Liu, L. Dai, L. You, W. Xu, and G. Qin, "Blueshift of electroluminescence from single n-inp nanowire/p-si heterojunctions due to the burstein–moss effect", Nanotechnology **19**, 465203 (2008).

[20]J. Wallentin, K. Mergenthaler, M. Ek, L. R. Wallenberg, L. Samuelson, K. Deppert, M.-E. Pistol, and M. T. Borgstrom, "Probing the wurtzite conduction band structure using state filling in highly doped inp nanowires", Nano letters **11**, 2286–2290 (2011).

[21]K. Mergenthaler, "Photon upconversion in heavily doped semiconductors", PhD thesis (Lund University, 2016).

[22]V. Heine, "Theory of surface states", Physical Review **138**, A1689 (1965).

[23]C. Mead and W. Spitzer, "Fermi level position at metal-semiconductor interfaces", Physical Review **134**, A713 (1964).

[24]J. Trägårdh, *Optical spectroscopy of single nanowires* (Lund University, 2008).

[25]Y.-S. Kang, D.-K. Kim, H.-K. Kang, K.-S. Jeong, M.-H. Cho, D.-H. Ko, H. Kim, J.-H. Seo, and D.-C. Kim, "Effects of nitrogen incorporation in hfo2 grown on inp by atomic layer deposition: an evolution in structural, chemical, and electrical characteristics", ACS applied materials & interfaces **6**, 3896–3906 (2014).

[26]A. C. Chia and R. R. LaPierre, "Analytical model of surface depletion in gaas nanowires", Journal of Applied Physics **112**, 063705 (2012).

[27]V. Schmidt, S. Senz, and U. Gösele, "Influence of the si/sio 2 interface on the charge carrier density of si nanowires", Applied Physics A **86**, 187–191 (2007).

[28]G. Nylund, *Studies of nanowire devices enabled by advanced nanofabrication* (Lund University, 2015).

[29]F. R. Chowdhury, S. Choudhury, F. Hasan, and T. Begum, "Optical properties of undoped and indium-doped tin oxide thin films", Journal of Bangladesh Academy of Sciences **35**, 99–111 (2011).

[30]T. Liu, X. Zhang, J. Zhang, W. Wang, L. Feng, L. Wu, W. Li, G. Zeng, and B. Li, "Interface study of ito/zno and ito/sno2 complex transparent conductive layers and their effect on cdte solar cells", International Journal of Photoenergy **2013** (2013).

[31]K. Storm, G. Nylund, M. Borgström, J. Wallentin, C. Fasth, C. Thelander, and L. Samuelson, "Gate-induced fermi level tuning in inp nanowires at efficiency close to the thermal limit", Nano letters **11**, 1127–1130 (2011).

[32]A. Mishra, L. Titova, T. Hoang, H. Jackson, L. Smith, J. Yarrison-Rice, Y. Kim, H. Joyce, Q. Gao, H. Tan, et al., "Polarization and temperature dependence of photoluminescence from zincblende and wurtzite inp nanowires", Applied Physics Letters **91**, 263104 (2007).

[33]Y.-H. Jeong, S. Takagi, F. Arai, and T. Sugano, "Effects on inp surface trap states of insitu etching and phosphorus-nitride deposition", Journal of applied physics **62**, 2370–2375 (1987).

[34]T. H. Gfroerer, "Photoluminescence in analysis of surfaces and interfaces", Encyclopedia of analytical chemistry: applications, theory and instrumentation (2006).

[35]G. Nylund, K. Storm, H. Torstensson, J. Wallentin, M. T. Borgström, D. Hessman, and L. Samuelson, "Transparently wrap-gated semiconductor nanowire arrays for studies of gate-controlled photoluminescence", in Aip conference proceedings, Vol. 1566, 1 (AIP, 2013), pp. 427–428.

[36]A. Liu and Y. Rosenwaks, "Excess carriers lifetime in inp single crystals: radiative versus nonradiative recombination", Journal of applied physics **86**, 430–437 (1999).

[37]G. A. Landis, P. Jenkins, and I. Weinberg, "Photoluminescence lifetime measurements in inp wafers", in [proceedings 1991] third international conference indium phosphide and related materials (IEEE, 1991), pp. 636–639.

[38]P. Dobal, H. Bist, S. Mehta, and R. Jain, "Laser heating and photoluminescence in gaas and al x ga1- x as", Applied physics letters **65**, 2469–2471 (1994).

[39]K. Sok Won, K. Manil, K. Inkoo, C. Minwoo, and R. Ji-Wook, "? optical properties of sputtered indium tin oxide thin films", Journal of Korean Physical Society **59**, 3280 (2011).

[40]L. Black, A. Cavalli, M. Verheijen, J. Haverkort, E. Bakkers, and W. Kessels, "Effective surface passivation of inp nanowires by atomic-layer-deposited al203 with po x interlayer", Nano letters **17**, 6287–6294 (2017).

[41]B. Simpkins, M. Mastro, C. Eddy Jr, and P. Pehrsson, "Surface depletion effects in semiconducting nanowires", Journal of Applied Physics **103**, 104313 (2008).

[42]J. Dow and R. Allen, "Surface defects and fermi-level pinning in inp", Journal of Vacuum Science and Technology **20**, 659–661 (1982).